

**AD-A213 924**

(4)

CONF

**APPROVED FOR PUBLIC RELEASE: DISTRIBUTION UNLIMITED**

**ANNUAL TECHNICAL REPORT**  
**(February 14, 1988 - February 14, 1989)**

entitled

**RESEARCH ON MERCURY CADMIUM TELLURIDE**

prepared for the

**Defense Advanced Research Projects Agency**

**SRF Contract No.: N00014-85-K-0151**

and administered by the

**Office of Naval Research**

**S.K. Gandhi**

**Electrical, Computer and Systems Engineering Department**

**Rensselaer Polytechnic Institute**

**Troy, New York 12180**

13  
89

**89 10 27 089**

UNCLASSIFIED

SECURITY CLASSIFICATION OF THIS PAGE

## REPORT DOCUMENTATION PAGE

1a. REPORT SECURITY CLASSIFICATION Unclassified			1b. RESTRICTIVE MARKINGS None		
2a. SECURITY CLASSIFICATION AUTHORITY None			3. DISTRIBUTION/AVAILABILITY OF REPORT Approved for public release; distribution unlimited		
2b. DECLASSIFICATION/DOWNGRADING SCHEDULE None					
4. PERFORMING ORGANIZATION REPORT NUMBER(S) N00014-85-K-0151-1			5. MONITORING ORGANIZATION REPORT NUMBER(S)		
6a. NAME OF PERFORMING ORGANIZATION Rensselaer Polytechnic Inst.		6b. OFFICE SYMBOL (If applicable) 3A707	7a. NAME OF MONITORING ORGANIZATION Office of Naval Research		
6c. ADDRESS (City, State and ZIP Code) 110 8th Street Troy, New York 12180-3590			7b. ADDRESS (City, State and ZIP Code) Resident Representative 715 Broadway, Fifth Floor New York, NY 10003-6896		
8a. NAME OF FUNDING/SPONSORING ORGANIZATION Defense Advanced Research Projects Agency		8b. OFFICE SYMBOL (If applicable)	9. PROCUREMENT INSTRUMENT IDENTIFICATION NUMBER N00014-85-K-0151-1		
8c. ADDRESS (City, State and ZIP Code) 1400 Wilson Boulevard Arlington, VA 22209			10. SOURCE OF FUNDING NOS.		
			PROGRAM ELEMENT NO. 61101E	PROJECT NO. YD14006	TASK NO. n/a
11. TITLE (Include Security Classification) RESEARCH ON MERCURY CADMIUM TELLURIDE					
12. PERSONAL AUTHOR(S) Sorab K. Ghandhi					
13a. TYPE OF REPORT Annual		13b. TIME COVERED FROM 2/15/88 TO 2/14/89		14. DATE OF REPORT (Yr., Mo., Day) August 1989	15. PAGE COUNT 64
16. SUPPLEMENTARY NOTATION Approved for public release; distribution unlimited					
17. COSATI CODES			18. SUBJECT TERMS (Continue on reverse if necessary and identify by block number)		
FIELD	GROUP	SUB. GR.	CdTe, ZnSe, HgCdTe, MCT, Epitaxy, MOCVD, OMVPE		
19. ABSTRACT (Continue on reverse if necessary and identify by block number) This report summarizes work done during the fourth year of a program entitled, "Research on Mercury Cadmium Telluride". Conventional growth of this material has been achieved with $\pm 0.001$ composition control over a 1" dia., using a rotating susceptor. A computer program has been written to evaluate anomalous Hall data. Techniques have been developed to achieve full annealing of these layers. Use of a new Te-alkyl has allowed growth of HgCdTe in the 250-320°C range.  Extrinsic p-doping of HgCdTe has been achieved, for the first time, in layers grown by OMVPE. Arsenic has been used as the acceptor, and its presence confirmed by SIMS data and by its stability with heat treatment (15 hours at 205°C).  The work was supported by the Defense Advanced Research Programs Agency (Contract monitor: Dr. J. Murphy), and administered through the Office of Naval Research (Dr. M. Yoder). Principal authors are Professors I.B. Bhat and S.K. Ghandhi.					
20. DISTRIBUTION/AVAILABILITY OF ABSTRACT UNCLASSIFIED/UNLIMITED <input checked="" type="checkbox"/> SAME AS RPT. <input type="checkbox"/> DTIC USERS <input type="checkbox"/>			21. ABSTRACT SECURITY CLASSIFICATION Unclassified		
22a. NAME OF RESPONSIBLE INDIVIDUAL Sorab K. Ghandhi			22b. TELEPHONE NUMBER (Include Area Code) 518-276-6085	22c. OFFICE SYMBOL	

**APPROVED FOR PUBLIC RELEASE: DISTRIBUTION UNLIMITED**

**ANNUAL TECHNICAL REPORT**  
**(February 14, 1988 - February 14, 1989)**

**entitled**

**RESEARCH ON MERCURY CADMIUM TELLURIDE**

**prepared for the**  
**Defense Advanced Research Projects Agency**  
**SRF Contract No.: N00014-85-K-0151**  
**and administered by the**  
**Office of Naval Research**

**S.K. Ghandhi**  
**Electrical, Computer and Systems Engineering Department**  
**Rensselaer Polytechnic Institute**  
**Troy, New York 12180**

**SK-89.44**

**September 5, 1989**

## CONTRIBUTORS

Professor I.B. Bhat (Full Time)

Dr. H. Ehsani (Part Time)

K.K. Parat (Doctoral Student)

N.R. Taskar (Doctoral Student)

D. Terry (Doctoral Student)

V. Natarajan (Doctoral Student)

J. Barthel (Tech. - Part Time)

A-1



## TABLE OF CONTENTS

### ABSTRACT

### 1. INTRODUCTION

### 2. WORK ACCOMPLISHED DURING THE PAST YEAR

#### 2.1 Reactor Development

#### 2.2 Growth of CdTe

#### 2.3 Growth of HgCdTe

##### 2.3.1 Low Temperature Growth

#### 2.4 Annealing Studies

#### 2.5 Extrinsic Doping Studies

#### 2.6 Lifetime Measurements

### 3. PAPERS AND PRESENTATIONS

### 4. PLANS FOR THE NEXT YEAR

### 5. ANTICIPATED PROBLEMS

APPENDIX A. Organometallic Vapor Phase Epitaxial Growth of HgTe and HgCdTe  
Using Methylallyltelluride

APPENDIX B. Extrinsic p-type Doping of HgCdTe Grown by Organometallic Epitaxy

APPENDIX C. The Organometallic Epitaxy of Extrinsic p-Doped HgCdTe

APPENDIX D. Computer Simulation Model for the Evaluation of Hall Data

## LIST OF FIGURES

- Figure 1 –  $R_H$  vs  $1000/T$  for a partially annealed sample
- Figure 2 –  $\sigma$  vs  $1000/T$  for a partially annealed sample
- Figure 3 –  $R_H$  and  $\sigma$  vs  $1000/T$  for a fully annealed sample
- Figure 4 – p-doping concentration vs arsine flow rate
- Figure 5 – Activation energy of arsenic vs acceptor concentration
- Figure 6 – Hall constant vs arsine flow
- Figure 7 – Arsenic signal for a HgCdTe layer with a CdTe cap and a CdTe buffer
- Figure 8 – Block diagram of microwave reflectance setup
- Figure 9 – Decay characteristic of HgCdTe layer

## ABSTRACT

Growth of HgCdTe has been carried out, using a new reaction chamber with a rotating susceptor. A compositional uniformity of  $\pm 0.001$  (Cd-fraction) has been obtained over a 1" diameter.

Low temperature growth of HgTe and HgCdTe have been achieved using methylalloytelluride as the tellurium source. This has allowed growth in the 250-320°C range with featureless morphology. Layers have an x-ray FWHM which is comparable to that of the substrate. Abruptness of the interface is also excellent, as evidenced by sharpness of pass-band fringes in the FTIR characteristic.

Extensive annealing studies have been carried out on HgCdTe layers. We have found that these are considerably harder to anneal than would be expected from bulk annealing data. A two temperature process has been developed to completely anneal these layers. A computer program, assuming a two-layer model, has been written to evaluate partially annealed layers, which have anomalous Hall characteristics. This has allowed separation of the surface and bulk characteristics of these layers.

P-type doping has been achieved, for the first time, in OMVPE grown HgCdTe. Doping levels to  $8 \times 10^{16}/\text{cm}^3$  have been obtained, using arsine gas as the arsenic source. Arsenic doping has been established by SIMS, and also by the fact that the doping level is unchanged after a 15 hour treatment at 205°C.

Lifetime measurements have been made using the technique of time domain reflectometry. This has allowed non-invasive measurements to be made on HgCdTe layers. Photoconductive devices have also been used to corroborate the data obtained from time domain reflectometry measurements.

## 1. INTRODUCTION

The goal of this program is to conduct research on Mercury Cadmium Telluride and related compounds. Its emphasis is on the growth of thin films of these materials by means of Organometallic Vapor Phase Epitaxy, and on their characterization. This report outlines tasks proposed and the accomplishments during the fourth year of our program.

## 2. WORK ACCOMPLISHED DURING THE PAST YEAR

### 2.1 Reactor Development

Our original reaction chamber, which used a stationary susceptor, was replaced during the last year with a new unit which has provisions for rotation. In addition, the reactor system was modified, and some of the gas channels reconfigured to allow for stable operation over long periods of time.

In this new system, the rotating platform is convectively heated by means of a fixed heating element, whose temperature is controlled by a feedback controller. As a result, temperature variations of the platform can occur due to the flow of hydrogen and chemical species over the substrate. The net result is that composition control over the time duration of a growth run was inadequate, as evidenced by a graded character to the FTIR transmission curve.

Many attempts were made to solve this problem by optimizing the controller parameters, and by minimizing substrate-heater clearances. The problem was eventually solved by redesigning the system so that the heater and the platform were integral units. Slip rings were used to provide power to this rotating system, and also to its imbedded thermocouple. This has proved completely satisfactory, as evidenced by a steep transition region in the FTIR curves taken on layers grown with the system.



Using this rotating heater, MCT layers have been grown with a  $\pm 0.001$  compositional uniformity over a 1" diameter. We are now in the process of making minor adjustments to the system, and hope to meet our goal of  $\pm 0.005$  variation over a 2" diameter slice during the coming year.

A total of 73 runs were made on this reactor during the last year. In addition, 121 runs were made on our research reactor. This machine, built in 1970, and perennially upgraded since then, continues to be useful in trying out new ideas with a rapid turn around time. Consequently, it is still in full use.

Mercury cadmium telluride (MCT) layers have been grown on bulk CdTe substrates, as well as on CdTeSe and CdTeZn substrates. Considerable work has been done on GaAs substrates as well.

Work has started on the construction of a new reactor, which incorporates many advanced design features. The concept for this machine was laid out last year. It has been designed as an extremely flexible unit, with high speed valves, pressure balancing, and full computer control. Two completely separate channels are provided, to allow growth by conventional as well as by atomic layer epitaxy.

The machine was originally developed to be used for HgCdTe. However, we have altered some aspects of the design in order to respond more closely to the recent DARPA shift in emphasis towards wide gap materials such as ZnSe and ZnTe. Provision has been made for the use of both conventional as well as pre-cracked sources, and also for the mechanical separation of species in a chamber with a rotating susceptor. The pressure balancing feature, combined with computer control, will allow the growth of superlattices as well as ternary alloys in this system.

At the present time, system construction has proceeded to the point where all of the input and exit plumbing are in place. Time and cost constraints have prevented the fabrication of the reaction chamber for now. It is our intention however, to keep this cham-

ber extremely simple at first, and construct the final version after some of the system characteristics have been worked out in preliminary runs.

## 2.2 Cadmium Telluride

A considerable amount of work has been carried out in past years on the development of high quality layers of CdTe, grown on InSb, to which it is closely lattice matched (0.07%). The resulting material is of excellent crystal quality, as evidenced by a photoluminescent peak with a FWHM of 2.1 meV at 12K, in undoped material. This value is the lowest reported for epitaxial CdTe grown by OMVPE. In addition, double crystal x-ray diffraction measurements on this material has resulted in a FWHM of 20 arc seconds, with coherent epitaxy for growth at 350°C.

Both p- and n-type extrinsic doping of these layers has been achieved, using AsH<sub>3</sub> and (C<sub>2</sub>H<sub>5</sub>)<sub>3</sub>In as the acceptor and donor dopant sources respectively. With both dopants, concentration levels up to  $1 \times 10^{17} \text{ cm}^{-3}$  to  $3 \times 10^{17} \text{ cm}^{-3}$  have been obtained. N-type layers, doped to  $8 \times 10^{15} \text{ cm}^{-3}$ , had a 300K Hall mobility value of 900 cm<sup>2</sup>/Vs and a 30K Hall mobility of 3500 cm<sup>2</sup>/Vs. This is comparable to values obtained for the best bulk CdTe with the same doping level.

A room temperature mobility of 80 cm<sup>2</sup>/Vs was measured for p-CdTe layers doped in the  $3 \times 10^{15}$  to  $3 \times 10^{16} \text{ cm}^{-3}$  range. The ionization energy of the arsenic acceptor was determined to be 62±4 meV, by means of variable temperature Hall and resistivity measurements.

Extrinsic doped junction diodes have been fabricated by successive growth of p- and n-layers on InSb substrates. Diodes have been shown to exhibit excellent characteristics, comparable to those obtained conventionally in GaAs devices. Typical characteristics are an ideality factor of 1.04 at a forward bias of 0.5V, a saturation current density of  $1.8 \times 10^{-12} \text{ A/cm}^2$ , and a leakage current of  $1.6 \times 10^{-11} \text{ A/cm}^2$ . These diodes were ex-

trinsically doped to  $1 \times 10^{17}/\text{cm}^3$  on both the p- and the n-side with arsenic and indium respectively. Light emission has also been measured from forward biased diodes of this type.

A number of experiments were devised to obtain some insight into the mechanism by which arsenic doping is so readily achieved in CdTe by OMVPE. In contrast, we note that this has only been achieved by laser excitation in MBE. One critical experiment which we have conducted is to attempt to dope CdTe using elemental arsenic which has been pre-cracked. Here, we could not achieve a hole concentration in excess of  $1 \times 10^{15}/\text{cm}^3$ , regardless of the partial pressure of the As species ( $\text{As}_2$  and  $\text{As}_4$ ).

The situation for arsenic incorporation from arsine is quite different; in fact, care must be taken to prevent excessive arsenic incorporation. Decomposition studies of this hydride (K. Tamaru, J. Phys. Chem., 59, 777, 1955) have established that the rate limiter is the removal of the first hydrogen atom, with subsequent hydrogen release being more rapid. Studies of  $\text{AsH}_3$  decomposition over CdTe have not been made. However, results with  $\text{AsH}_3$  over GaAs indicate that decomposition occurs at temperatures as low as  $172^\circ\text{C}$ , by a surface catalyzed reaction. We propose, therefore, that  $\text{AsH}_3$  breaks down to  $\text{AsH}_2$  and is chemisorbed on the CdTe surface, where further loss of the remaining two hydrogens results in its decomposition to monatomic As. This Column 5 atom incorporates into Te (Column 6) sites which are electronically favored over Cd (Column 2) sites. As a consequence, the As incorporation can be altered by changing DMTe overpressure during growth. Thus, increasing this overpressure reduces the Te-vacancy concentration, resulting in a fall in the p-doping concentration. We have demonstrated that this is indeed the case, with an inverse dependence, as predicted.

The situation with  $\text{As}_2$  is probably quite different, since its incorporation as a p-dopant would necessitate the substitution of one As atom into a Te-site, followed by the breaking of the As-As bond. This is not readily achieved at growth temperatures, so

that it is entirely possible for the second As to be incorporated into a neighboring Cd site, where it would behave as a triple donor, and compensate the CdTe. We note that the bond strength of As-As is extremely large (92 kcal/mole), so that the breaking of this bond is probably the rate limiter to the doping process when elemental arsenic is used.

We conclude, therefore, that it is necessary to provide atomic arsenic to the CdTe in order to promote its ready incorporation into the CdTe lattice. The use of the hydride  $\text{AsH}_3$  allows this to be done in a convenient manner. A variety of arsenic alkyls can also be successful for this doping process, provided their eventual decomposition to As-H is surface catalyzed. Tertiarybutylarsenic is a likely candidate for this reason; on the other hand, trimethylarsenic would probably be a poor choice since it does not decompose to As-H.

### 2.3 Growth of Mercury Cadmium Telluride

The growth of undoped HgCdTe is now a routine matter in our laboratory, and is carried out on CdTe, CdTeZn and CdTeSe substrates. Our results on the lattice matched materials are generally superior to those on CdTe; however, many of our studies are made on CdTe because of its more ready availability. In some instances, as in x-ray studies where the substrate lattice parameter is critical, we are certainly very particular about our choice of the substrate material.

Typically, most of the undoped material which we grow is on  $1 \text{ cm} \times 1 \text{ cm}$  substrates, in the range of  $x = 0.2$  to  $0.28$ . We prefer to use material in the  $x = 0.23$  composition range for many of our characterization studies, since the mobility of  $x = 0.2$  layers is strongly affected by small changes in composition. Thus, it is more easy to carry out studies on material with slightly higher composition values.

All of our layers are grown in a vertical reactor, at a substrate temperatures of

370°C, by the simultaneous pyrolysis of dimethylcadmium, diisopropyltellurium and elemental mercury in hydrogen gas. The growth rate for these layers is about 3.5  $\mu\text{m/hr}$ .

HgCdTe layers are capped with a 0.5 to 1  $\mu\text{m}$  thick layer of undoped CdTe which is grown in the same reactor run. This cap prevents unintentional annealing of the layers during the cool down period. As a result, as-grown layers have an acceptor concentration of about  $3 \times 10^{16}/\text{cm}^3$  due to mercury vacancies.

Fourier transform infrared (FTIR) transmission spectroscopy is used to measure layer thickness and compositional uniformity across the wafer. This technique is nondestructive, and has a sensitivity which is comparable to or better than that obtained by alternative methods, such as energy dispersive x-ray analysis. Typically, layers grown with the stationary susceptor have edge to edge compositional uniformity (Cd fraction) of better than  $\pm 0.005$  over a 1 cm  $\times$  1 cm area. Recently, the shift to a rotating susceptor has resulted in a  $\pm 0.001$  compositional uniformity over a 1" diameter. The thickness uniformity of the layer is also excellent, better than  $\pm 0.7 \mu\text{m}$  for 12- $\mu\text{m}$  thick layers.

Layers of comparable uniformity can also be grown by using an interdiffused multilayer process (IMP), where alternate layers of CdTe and HgTe are grown under conditions which have been optimized for each binary compound, and homogenized at the growth temperature with an annealing step. The crystallinity of interdiffused HgCdTe has been shown to be poorer than that of alloy grown HgCdTe, as determined by double crystal x-ray diffraction. This is seen in Table 1, from S.J.C Irvine et al., J. Vac. Sci. Technol. A7(2) 285 (1989). In this table, the lowest value for x-ray FWHM, 47-51 arc-sec, is for 6  $\mu\text{m}$  thick samples, grown by us on lattice matched substrates. The IMP data given here is for 12  $\mu\text{m}$  thick layers, by way of comparison.

### 2.3.1 Low Temperature Growth of HgCdTe

HgCdTe (MCT) is very susceptible to thermally induced defects at the growth tem-

TABLE I. Comparison of epitaxial CMT crystallographic quality.

Layer structure	Growth technique	x-ray FWHM (arc s)	Reference
CMT ( $x = 0.3$ )/CdTe/ $\text{Al}_2\text{O}_3$	MOVPE	72-150	3
CMT ( $x = 0.3$ )/CdTe/ $\text{Al}_2\text{O}_3$	IMP	150-210	3
CMT ( $x = 0.3$ )/CdTe/ $\text{Al}_2\text{O}_3$	LPE	78-108	3
CMT ( $x = 0.22$ )/CdTe	MOVPE (IMP)	67-135 $9 \times 7.5$ mm	Present work
CMT ( $x = 0.235$ )/CdTe/GaAs	MOVPE (IMP)	< 84 $8 \times 8$ mm (best 55)	Present work
CMT ( $x = 0.18$ )/CdTe	MOVPE	151 $\pm$ 15	4
CMT ( $x = 0.2$ )/CdTe/GaAs	MOVPE	110	12
CMT ( $x = 0.182$ )/CdSe <sub>0.04</sub> Te <sub>0.96</sub>	MOVPE	47-51	4
CMT ( $x = 0.20$ )/CdZnTe	MBE	65 $10 \times 10$ mm (best 26)	13

perature. Thus, significant improvements can be realized if growth is carried out at reduced temperature. Many approaches, using laser, UV and plasma excitation have been proposed for this purpose. We believe that the approach of using Te alkyls, which are more readily cracked, is the most promising one. Historically, diethyltelluride (DETe) was used for the OMVPE of HgCdTe, at a growth temperature of 415°C, to achieve a reasonable growth rate (around 3-4  $\mu\text{m/h}$ ). More recently, the use of diisopropyltelluride (DIPTe) has allowed the growth temperature to be reduced to around 370°C, while maintaining this growth rate. Other Te precursors such as di-*tert*-butyltelluride and diallyltelluride have been used to grow HgTe or CdTe at low temperatures (250-350°C). A disadvantage of these chemicals is their low vapor, which necessitates the use of heated bubblers and lines to transport a sufficient amount of Te to the reactor. Table 2 lists a number of these tellurium sources, and indicates the variety that is available for the growth of HgCdTe at the present time.

During the past year we have investigated the growth of HgCdTe using methylallyltelluride (MATE) as the tellurium alkyl. This source has the advantage of relatively high vapor pressure (6.2 Torr at 20°C) so that it can be transported readily to the reaction zone.

The epitaxial growth of HgTe and HgCdTe was carried out at reduced pressure (380 Torr) in a vertical reactor using MATE, DMCd, and Hg as the Te, Cd, and Hg sources respectively. Both HgTe and HgCdTe layers were grown in the temperature range from 250-320°C, with growth rates comparable to those obtained at 50°C higher temperatures using DIPTe. Results of this study are detailed in Appendix A and B at the end of this report. By way of summary, we found that:

- a) layer morphology was considerably improved over what is normally obtained with DIPTe, with a complete absence of step features.
- b) the x-ray full width half maximum for HgTe (29 arc sec) closely approached that of

TABLE 2

## ORGANOMETALLIC TELLURIUM SOURCES

Compound	Acronym	$T_{growth}$
Dimethyltelluride $(CH_3)_2Te$	DMTe	$\simeq 450^\circ C$
Diethyltelluride $(C_2H_5)_2Te$	DETe	$\simeq 415^\circ C$
Diisopropyltelluride $(C_3H_7)_2Te$	DIPTe	$\simeq 350^\circ C$
Dimethylditelluride $(CH_3)_2Te_2$	DMDTe	$\simeq 300^\circ C$
Methylallyltelluride $C_4H_8Te$	MATe	$\simeq 300^\circ C$
Diallyltelluride $(C_3H_5)_2Te$	DATe	$\simeq 300^\circ C$
Methyltertiarybutyltelluride $C_5H_{12}Te$	MTBTe	$\simeq 300^\circ C$
Ditertiarybutyltelluride $(C_4H_9)_2Te$	DTBTe	$\simeq 300^\circ C$



the lattice matched CdTeZn substrate (28 arc sec) on which it was grown. This was true, even for very thin ( $1.7\ \mu\text{m}$ ) layers.

- c) the Fourier transform infrared spectrum of the band-edge region, for layers grown on a CdTe substrate, show excellent epilayer substrate interface abruptness as demonstrated by the sharp fringes present, even for thin ( $3.3\ \mu\text{m}$ ) layers. The interference fringes of the FTIR spectra of  $3\ \mu\text{m}$  thick layers grown using DIPTe at  $370^\circ\text{C}$  were found to be less sharp, due to interdiffusion effects at the interface. Finally,
- d) the long-wavelength FTIR characteristic of extremely thin ( $1.7\ \mu\text{m}$ ) layers, grown at  $325^\circ\text{C}$  using MATe, exhibited sharp fringes associated with the difference in refractive indices of the epilayer and the substrate. These are indicative of the abruptness of the interface.

The results of this initial study have served to emphasize the advantage of growth at a somewhat lower temperature than what we have conventionally used for HgCdTe layer growth. Further work along these lines is presently being undertaken. However, it should be emphasized that considerably more work will have to be done if HgCdTe, grown by this technique, can be fully characterized for suitability as focal plane array material.

## 2.4 Annealing Studies

The annealing behavior of HgCdTe has been investigated in detail during the last year. Typically, our as-grown layers, which are p-type with carrier concentrations around  $1\text{-}2 \times 10^{16}/\text{cm}^3$  due to mercury vacancies, become light p-type with carrier concentrations around  $1\text{-}2 \times 10^{15}/\text{cm}^3$  after Hg saturated annealings at temperatures in the range of  $200\text{-}230^\circ\text{C}$ . These conditions, usually sufficient for the complete annealing of bulk  $\text{Hg}_{1-x}\text{Cd}_x\text{Te}$  to n-type, are thus inadequate for OMVPE grown epilayers. This

problem has been encountered in layers grown by LPE and MBE as well.

During our work, we have developed a new annealing technique which allows successful conversion of these layers to n-type. We have found that the as-grown layers are converted to n-type, with a carrier concentration of approximately  $5 \times 10^{14}/\text{cm}^3$ , by a higher temperature anneal around 270-290°C, followed by a low temperature anneal at 220°C.

With bulk HgCdTe, Hg from the vapor diffuses into the crystal during annealing, possibly via an interstitial mechanism. Subsequently, the Hg interstitials become substitutional by moving into vacant Hg sites. Thus,  $[V_{Hg}]$  is a function of the annealing temperature as well as the concentration of Hg interstitials,  $[I_{Hg}]$ , which are present in the lattice at the annealing temperature. In turn,  $[I_{Hg}]$  is a function of the annealing temperature as well as the Hg overpressure.  $[V_{Hg}]$  can thus be controlled in HgCdTe, by controlling the annealing temperature as well as the Hg overpressure. Values of  $[V_{Hg}]$  as a function of these annealing parameters are available in the literature for different values of  $x$ . An effective diffusion coefficient of Hg into HgCdTe, relevant to the annealing process, has also been given. However, most of the annealing results reported in the literature have been on bulk materials.

The annealing characteristics of HgCdTe layers, grown by epitaxial techniques such as liquid phase epitaxy (LPE) and organometallic vapor phase epitaxy (OMVPE), are less understood. Moreover, they are quite different from those reported for bulk material. As-grown layers are typically p-type due to the low Hg vapor pressures used during the growth of OMVPE layers, and the higher temperatures employed in the growth of LPE layers. The reduction of Hg vacancies thus requires a low temperature Hg saturated anneal. In the case of LPE, some authors have noted that complete annealing of layers with alloy compositions greater than 0.20 was not possible. With OMVPE layers, extremely long anneal times (21 days) have been used to completely anneal a 10

$\mu\text{m}$  layer of  $\text{HgCdTe}$ . Additionally, higher temperature anneals have been used for completely annealing these layers. All of this work has focused on fully annealed layers; however, it is necessary to investigate the behavior of partially annealed layers in order to gain an understanding of their annealing behavior.

All layers grown for our annealing studies were capped with a 0.5-1.0  $\mu\text{m}$  thick layer of undoped  $\text{CdTe}$  which was grown in the same reactor run. This cap serves two purposes; first, it prevents any unintentional annealing of the  $\text{HgCdTe}$  layers during cool-down after the layer growth. Second, it inhibits the formation of an inversion layer on the  $\text{HgCdTe}$  surface, which can affect the Hall characterization of as-grown p-type layers. Cap layers were removed just prior to the annealing by means of a short etch consisting of 1%  $\text{Br}$  in methanol. The epilayer thickness was determined from the interference fringes in the sub-bandgap regime of the IR transmittance curve. The bandgap of the layer was taken to be the energy at which the absorption coefficient of the material is  $500\text{ cm}^{-1}$ , and then used to determine the alloy composition.

After cap removal, samples were rinsed in methanol, dried with nitrogen, and loaded in an aqua regia cleaned quartz ampoule with mercury of 99.99999% purity. The ampoule was evacuated to  $10^{-7}$  Torr using a turbo-molecular pump equipped with a liquid nitrogen trap, and sealed using an oxy-hydrogen flame. All annealings were carried out with the sample kept  $2^\circ\text{C}$  warmer than the  $\text{Hg}$  reservoir, to avoid  $\text{Hg}$  from condensing on them. This prevented any surface deterioration during the anneal and sample surfaces showed no sign of damage. The annealed samples were characterized by van der Pauw techniques without any further surface treatment.

A number of the samples showed anomalous behavior. This comes about because of an n-type surface accumulation layer on the p-epilayer. Characterization of these samples is best done by fitting the Hall data from 300 to 10 K, to a computer simulation which assumes the presence of these two layers. This computer simulation model is de-

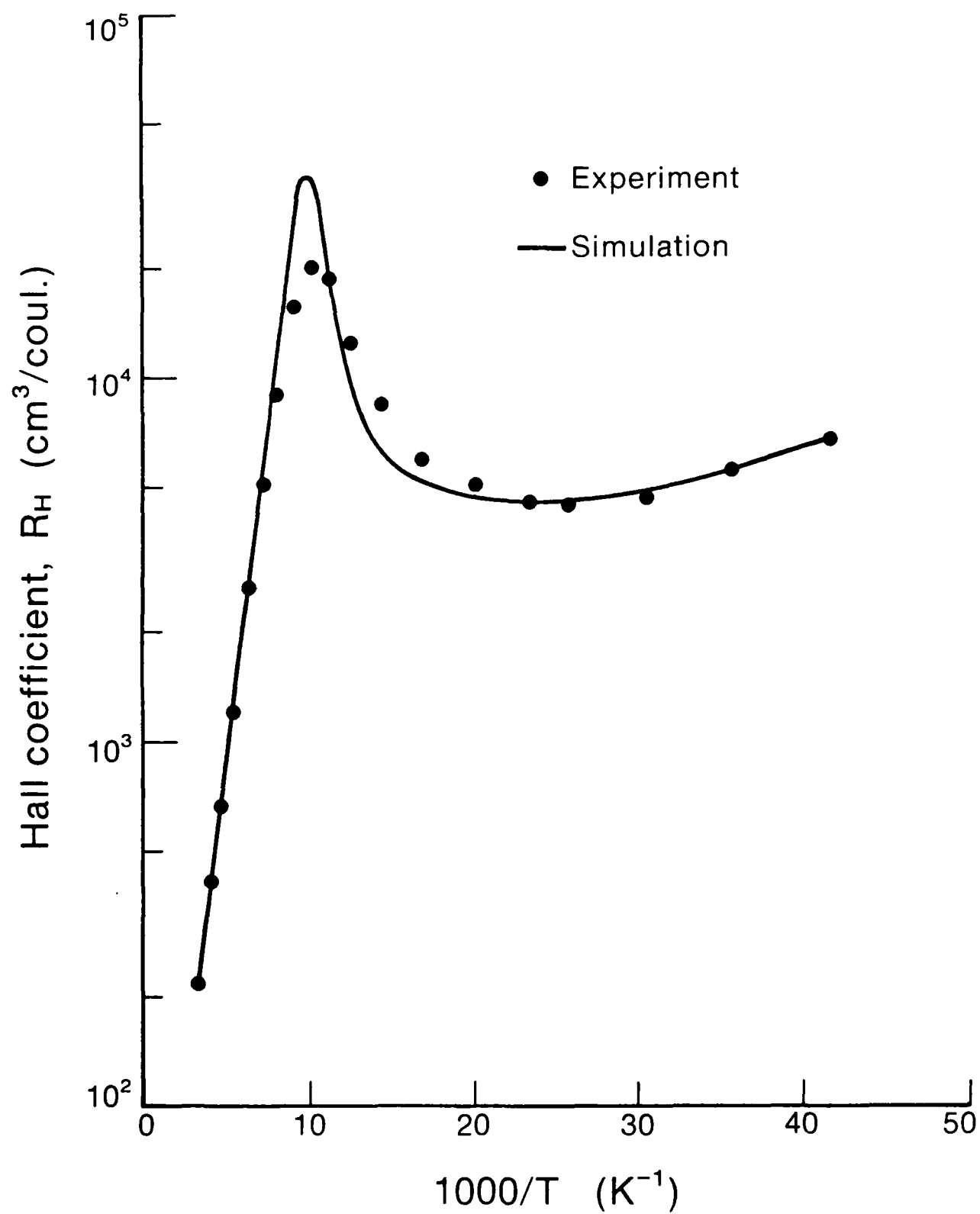


Figure 1.  $R_H$  vs  $1000/T$  for a partially annealed sample.

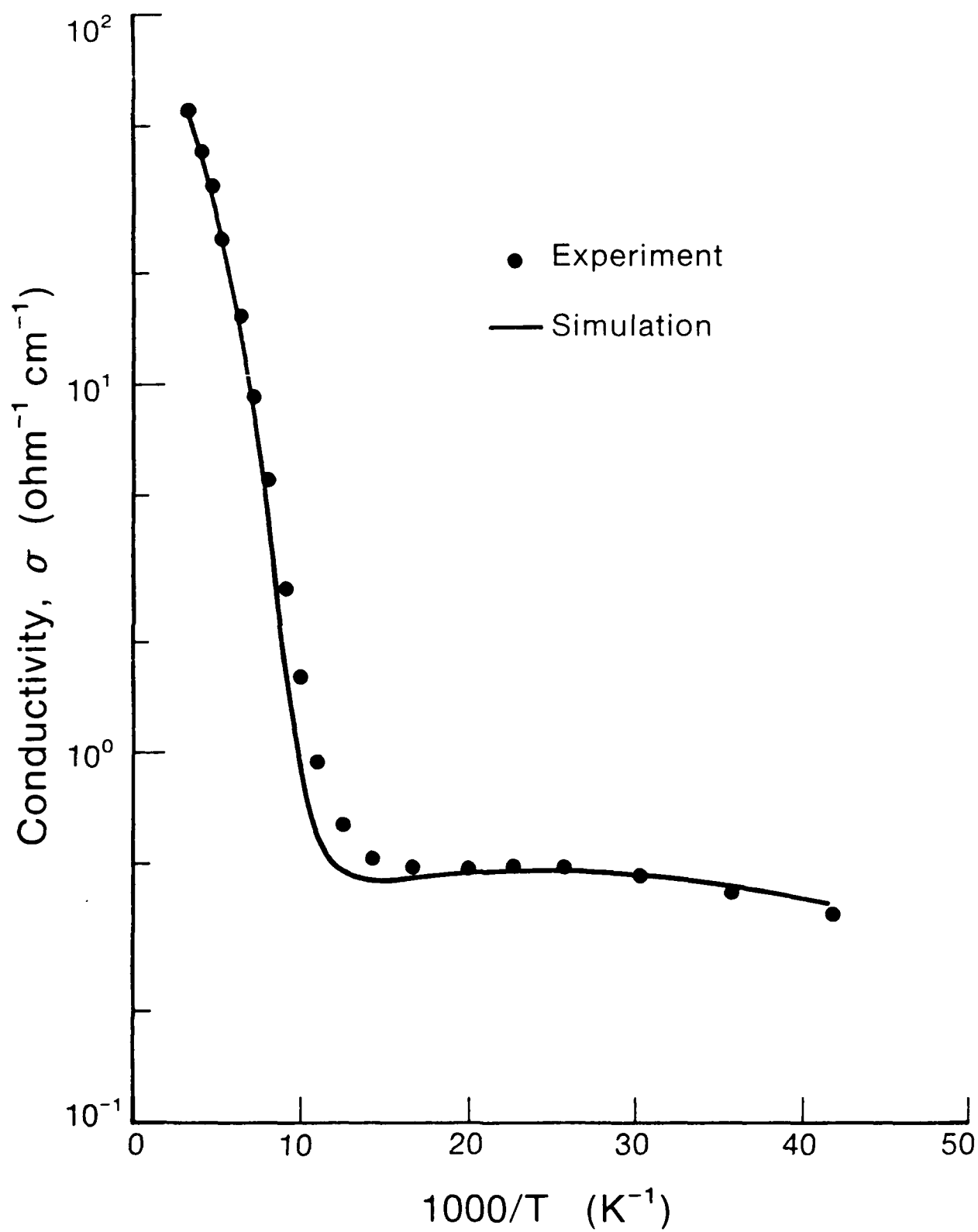


Figure 2.  $\sigma$  vs 1000/T for a partially annealed sample.

scribed in Appendix D. For some of the samples which exhibited anomalous behavior, the surface was passivated by anodic sulfidization, and the Hall data taken once again. This served to reduce the effect of the accumulation layer on the Hall characteristics.

As-grown layers showed classical Hall behavior. For a typical  $6.7 \mu\text{m}$  layer with  $x = 0.228$ , the best fit corresponded to  $(N_A - N_D)$  of  $3.61 \times 10^{16}/\text{cm}^3$ , a hole ionization energy of  $6.2 \text{ meV}$ , and a low temperature hole mobility ( $\mu_{po}$ ) of  $840 \text{ cm}^2/\text{Vs}$ . It was not necessary to consider the presence of any inversion layer in order to obtain this fit.

Figures 1 and 2 show the  $R_H$  and  $\sigma$  versus  $1000/T$  of a sample annealed at  $230^\circ\text{C}$  for 9 hours, taken at  $2.1 \text{ kG}$ . This sample had an  $x$  value of  $0.208$  and a thickness of  $12 \mu\text{m}$ . This combination of temperature and time should be sufficient to anneal bulk  $\text{HgCdTe}$  up to a depth of  $15 \mu\text{m}$ . Here, the complete conversion of the epilayer is not achieved as evidenced from the anomalous Hall characteristics. The  $R_H$  and  $\sigma$  curves were fitted assuming a p-type epilayer with n-type surface inversion. Parameters providing the best fit (represented by the solid curves) are  $N_A$  of  $1.65 \times 10^{15}/\text{cm}^3$ ,  $N_D$  of  $4 \times 10^{15}/\text{cm}^3$ ,  $E_A$  of  $6.9 \text{ meV}$  and a low temperature hole mobility ( $\mu_{po}$ ) of  $1620 \text{ cm}^2/\text{Vs}$  for the bulk layer. The inversion layer carrier concentration was  $2.2 \times 10^{11}/\text{cm}^2$ , with a low temperature surface electron mobility ( $\mu_{so}$ ) of  $7000 \text{ cm}^2/\text{Vs}$ .

The fact that this was indeed a p-type layer with surface inversion was verified by sulfidizing the sample in an anodic bath. This anodic sulfide is expected to have a low concentration of fixed positive charges in it, and hence should reduce the inversion layer concentration at the surface. Computer simulation of the Hall data was made, using the same bulk parameters as given earlier. Now, however, best fit was achieved when the surface carrier concentration was reduced to  $1.3 \times 10^9/\text{cm}^2$  and the inversion layer mobility increased to  $33,000 \text{ cm}^2/\text{Vs}$ . This increase in surface mobility is expected, since passivation tends to reduce surface scattering effects.

Data on a number of partially annealed samples is shown in Table 3.

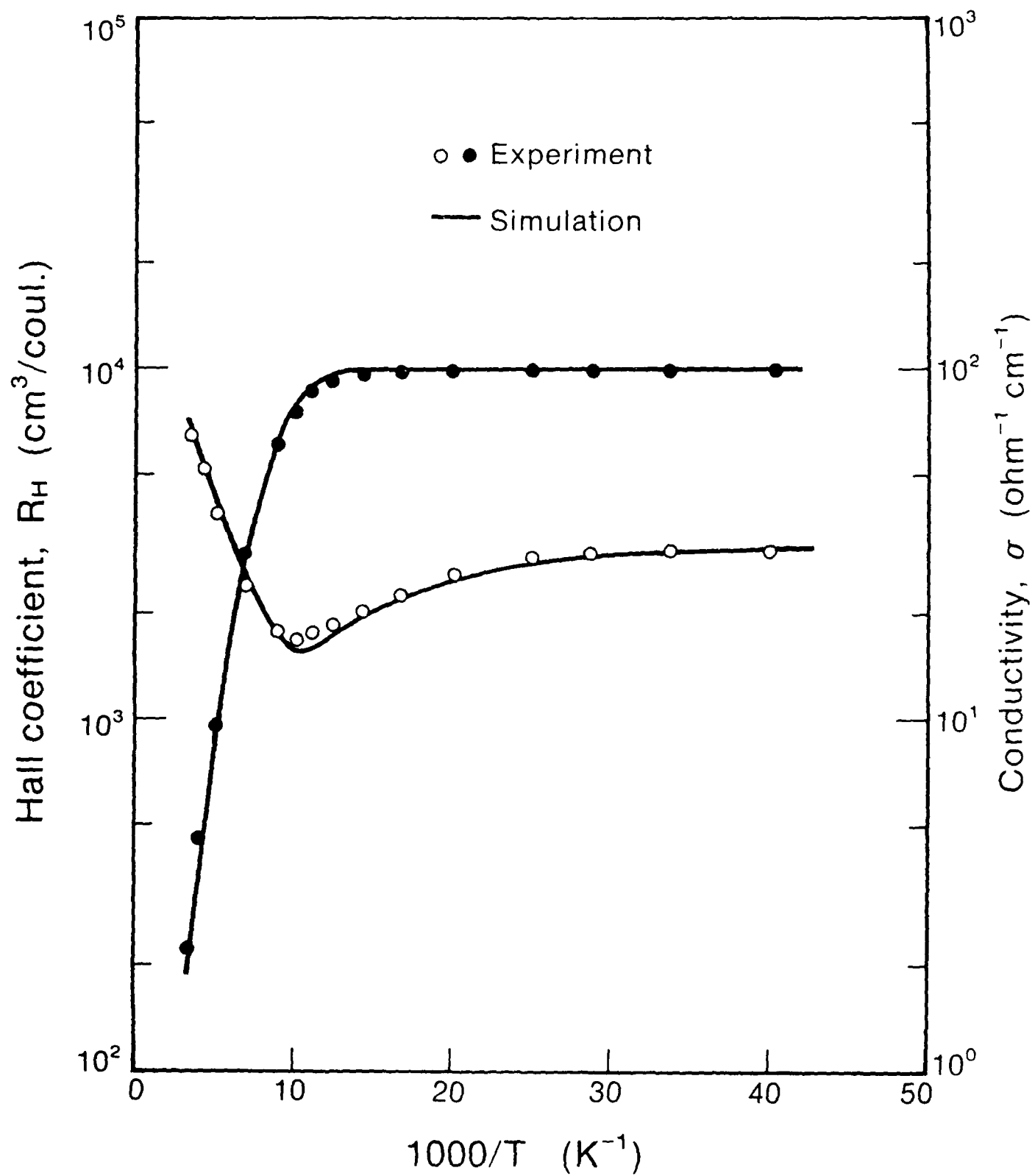


Figure 3.  $R_H$  and  $\sigma$  vs  $1000/T$  for a fully annealed sample.

TABLE 3

Sample	$x$	Thickness ( $\mu\text{m}$ )	Annealing Conditions	$(N_A - N_D)$ ( $\text{cm}^{-3}$ )
1.	0.228	6.7	unannealed	$3.61 \times 10^{16}$
2.	0.219	6.3	$205^\circ\text{C}/24 \text{ hr.}$	$6.5 \times 10^{14}$
3.	0.208	12.0	$230^\circ\text{C}/9 \text{ hr.}$	$1.25 \times 10^{15}$
4.	0.204	11.4	$230^\circ\text{C}/24 \text{ hr.}$	$0.7 \times 10^{14}$
5.	0.232	13.0	$240^\circ\text{C}/12 \text{ hr.}$	$5.0 \times 10^{14}$

In all cases, the layers are still weakly p-type, after anneal cycles as long as 24 hours at  $230^\circ\text{C}$ . Also shown, for comparison, is an as-grown sample, i.e., one which has not been annealed. This sample is heavily p-type as expected.

Figure 3 shows  $R_H$  and  $\sigma$  versus  $1000/T$  for a sample annealed at  $290^\circ\text{C}$  for 15 hours, followed by a  $220^\circ\text{C}$  anneal for 13 hours. The layer was  $8.2 \mu\text{m}$  thick, with  $x = 0.205$ . The data were taken at 1.1 kG. It is seen from the shape of the  $R_H$  curve, that this is an n-type layer. However, it is possible that the measured electron concentration and mobility are different from the actual bulk electron concentration and mobility, due to the presence of the surface electrons. Using computer simulation, the following bulk and surface parameters provided the best fit to the measured Hall data:  $(N_D - N_A)$  of  $5.4 \times 10^{14}/\text{cm}^3$ ,  $N_s$  of  $2.4 \times 10^{11}/\text{cm}^2$ , a low temperature bulk electron mobility ( $\mu_{no}$ ) of  $380,000 \text{ cm}^2/\text{Vs}$  and a surface electron mobility ( $\mu_{so}$ ) of  $30,000 \text{ cm}^2/\text{Vs}$ . Table 4 lists the results of Hall data on this and several other annealed samples, which show complete conversion to n-type.



TABLE 4

Sample	$x$	Thickness ( $\mu\text{m}$ )	Annealing Conditions	$(N_D - N_A)$ ( $\text{cm}^{-3}$ )	$\mu_n(30K)$ ( $\text{cm}^2/\text{V-s}$ )
1.	0.205	8.2	290°C/15 hr. +220°C/13 hr.	$5.4 \times 10^{14}$	334,000
2.	0.220	5.8	290°C/15 hr. +220°C/13 hr.	$6.2 \times 10^{14}$	210,000
3.	0.226	5.8	290°C/15 hr. +220°C/13 hr.	$3.3 \times 10^{14}$	120,000
4.	0.226	5.8	270°C/14 hr. +220°C/12 hr.	$3.5 \times 10^{14}$	190,000
5.	0.224	4.5	270°C/14 hr.	$1.0 \times 10^{14}$	110,000

The last sample in this table shows the result for annealing at 270°C for 14 hours, followed by quenching to room temperature. This was done in order to check the suitability of a single high temperature step for complete annealing of the HgCdTe layer. Here, the residual donor concentration is  $1 \times 10^{14}/\text{cm}^3$ . However, compared to other samples in this table, one would expect a net donor concentration of approximately  $5 \times 10^{14}/\text{cm}^3$ , and a considerably higher value of electron mobility. The discrepancy is probably due to the fact that  $[V_{Hg}]$  is about  $4 \times 10^{14}/\text{cm}^3$  for a 270°C Hg saturated anneal. This would compensate the residual donor concentration of around  $5 \times 10^{14}/\text{cm}^3$ , reducing the net carrier concentration to the  $1 \times 10^{14}/\text{cm}^3$  range. A low temperature anneal around 220°C, on the other hand, results in  $[V_{Hg}]$  in the low  $1 \times 10^{13}/\text{cm}^3$  range, thus reducing the compensation. This indicates the advantage of a two-step anneal, with a higher temperature anneal followed by a low temperature anneal.

We believe that the annealing behavior of HgCdTe can be explained by considering the role of Te precipitates in the annealing process, and propose a tentative model

to this effect. Interstitial Hg is expected to react readily with these precipitates, the reaction rate being limited by the mass transport of the Hg to the Te precipitate, which act as a sink for this Hg. During the annealing process, the diffusion length of interstitial Hg is comparable to the spacing between the Te precipitates, resulting in an overall lowering of  $[I_{Hg}]$  in the lattice. This would cause a higher concentration of vacancies to exist in the lattice as long as the Te precipitates are present, since  $[V_{Hg}]$  is inversely proportional to  $[I_{Hg}]$ . Once the Te precipitates are all annihilated,  $[I_{Hg}]$  can rise to its equilibrium value, and  $[V_{Hg}]$  drops to the value quoted in the literature for Hg saturated anneals at these temperatures. This would explain why there is a persistence of vacancies in the lattice in spite of the annealing. A higher temperature annealing enhances the in-diffusion of Hg, and increases the rate of annihilation of the Te precipitates. This, followed by a low temperature anneal, will reduce the Hg vacancies and convert the layer to n-type. A study of the role of Te precipitates in these layers is currently being undertaken.

It is also possible that the discrepancy is caused by some forms of stoichiometric defect other than Te precipitates, which are not annealed out during the low temperature anneal. A higher temperature may be required for dissolving these defects.

## 2.5 Extrinsic Doping Studies

With HgCdTe, as grown material is generally p-type due to the presence of native defects such as mercury vacancies, provided that the residual (donor) impurities in the starting chemicals are in very low concentration. This material, with its doping concentration adjusted by annealing at an appropriate temperature, is commonly used in detector arrays of the p-n junction type. Instead of relying on stoichiometry control, however, it is desirable to introduce external impurities during growth to get p-type layers. This is because native defects are relatively deep compared to shallow impurities, so that the

lifetime of this material is correspondingly shorter. Elements from group III and group VII behave as n-type dopants and elements from group I and group V act as p-type. For p-doping, group V elements are preferred over Group I because they are much slower diffusing acceptors and hence can be used to form stable device structures.

Doping of HgCdTe by group V elements such as Sb, As and P has not been very successful by many growth methods. For example, As and Sb doping by liquid phase epitaxy (LPE) from Te-rich solutions does not always result in p-type layers, even after the Hg vacancy concentration is reduced by a low temperature anneal in a Hg-rich ambient.

P-type doping has not been achieved in HgCdTe layers grown by the interdiffused multilayer process (IMP). This is because the incorporation efficiency of As in CdTe is orders of magnitude larger than in HgTe. As a result, arsenic doping occurs in striations, over 20% of the layer thickness (for  $x = 0.2$ ). This arsenic does not homogenize throughout the layer during subsequent heat treatment because it is a slow diffuser. In molecular beam epitaxy (MBE), both Sb and As behave as n-type dopants.

During the past year we have demonstrated, for the first time, that p-type doping can be achieved in HgCdTe, using arsenic (in the form of  $\text{AsH}_3$ ) as the dopant source. In our experiments, many undoped layers were first grown in order to determine the background doping level. This was necessary in order to separate out the doping effect due to Hg vacancies from that of the intentional dopant, As. All the layers grown in this reactor, without any intentional doping, were weakly n-type (in the low  $10^{15} \text{ cm}^{-3}$  range). Typical parameters for such layers are  $x = 0.3$ ;  $n = 3.5 \times 10^{15} / \text{cm}^3$  and  $\mu = 2.4 \times 10^4 \text{ cm}^2 / \text{Vs}$  at 40K. All layers were grown on GaAs substrates with a 2-3  $\mu\text{m}$  CdTe buffer layer.

Arsenic doped HgCdTe layers on GaAs were grown with p-doping levels in the range  $3.5 \times 10^{15} \text{ cm}^{-3}$  to  $4.3 \times 10^{16} \text{ cm}^{-3}$ . No evidence of surface inversion was observed

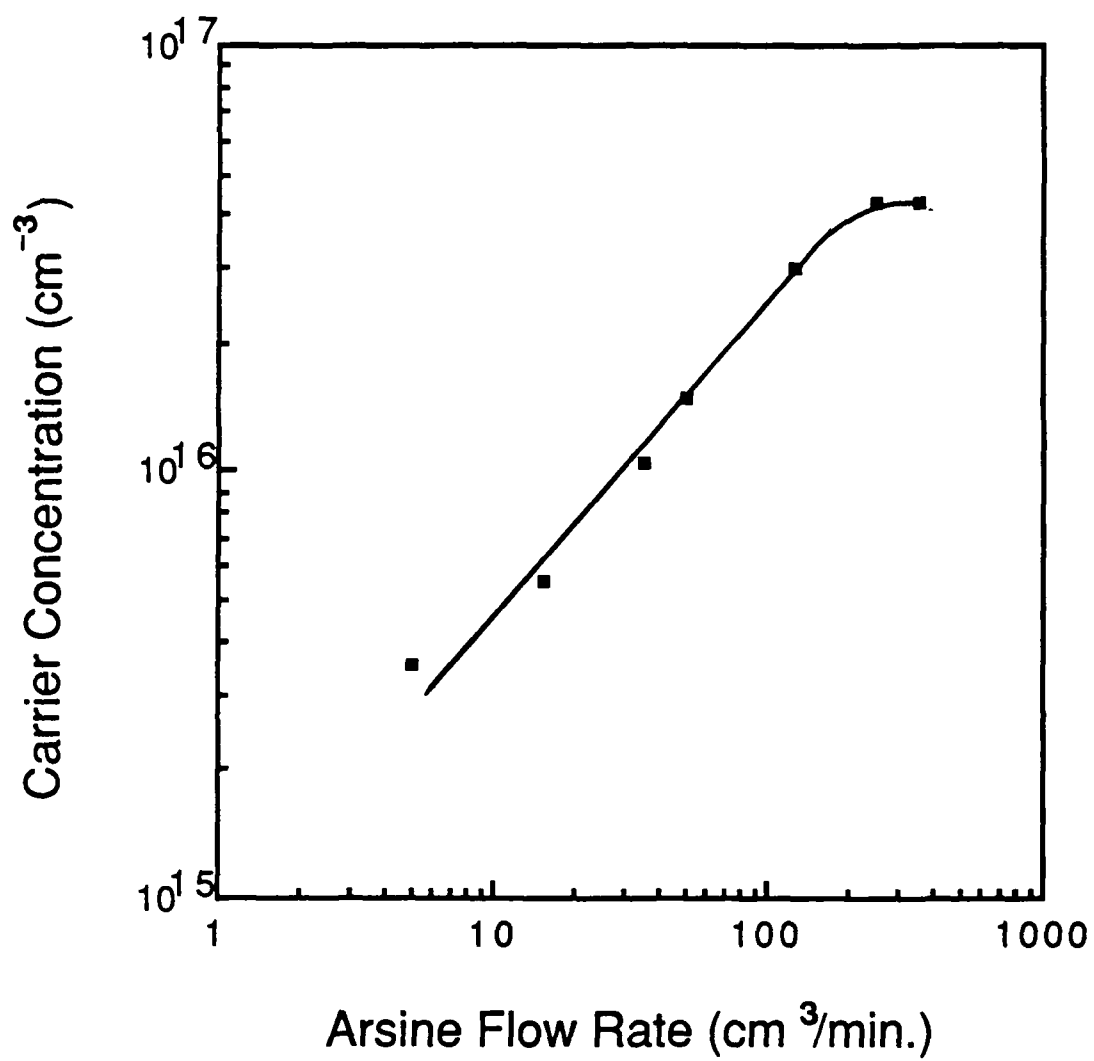


Figure 4. p-doping concentration vs. arsine flow rate.

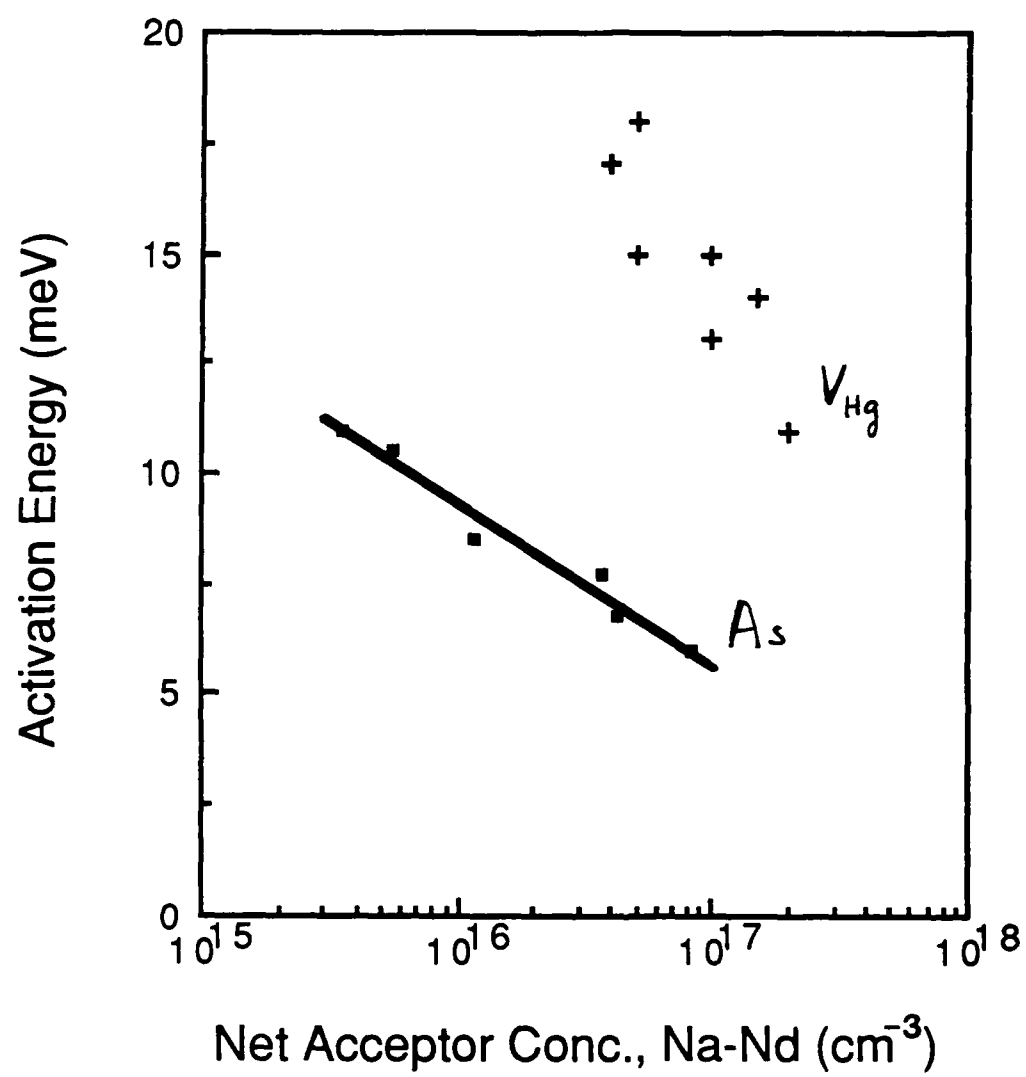


Figure 5. Activation energy of arsenic vs. acceptor concentration.

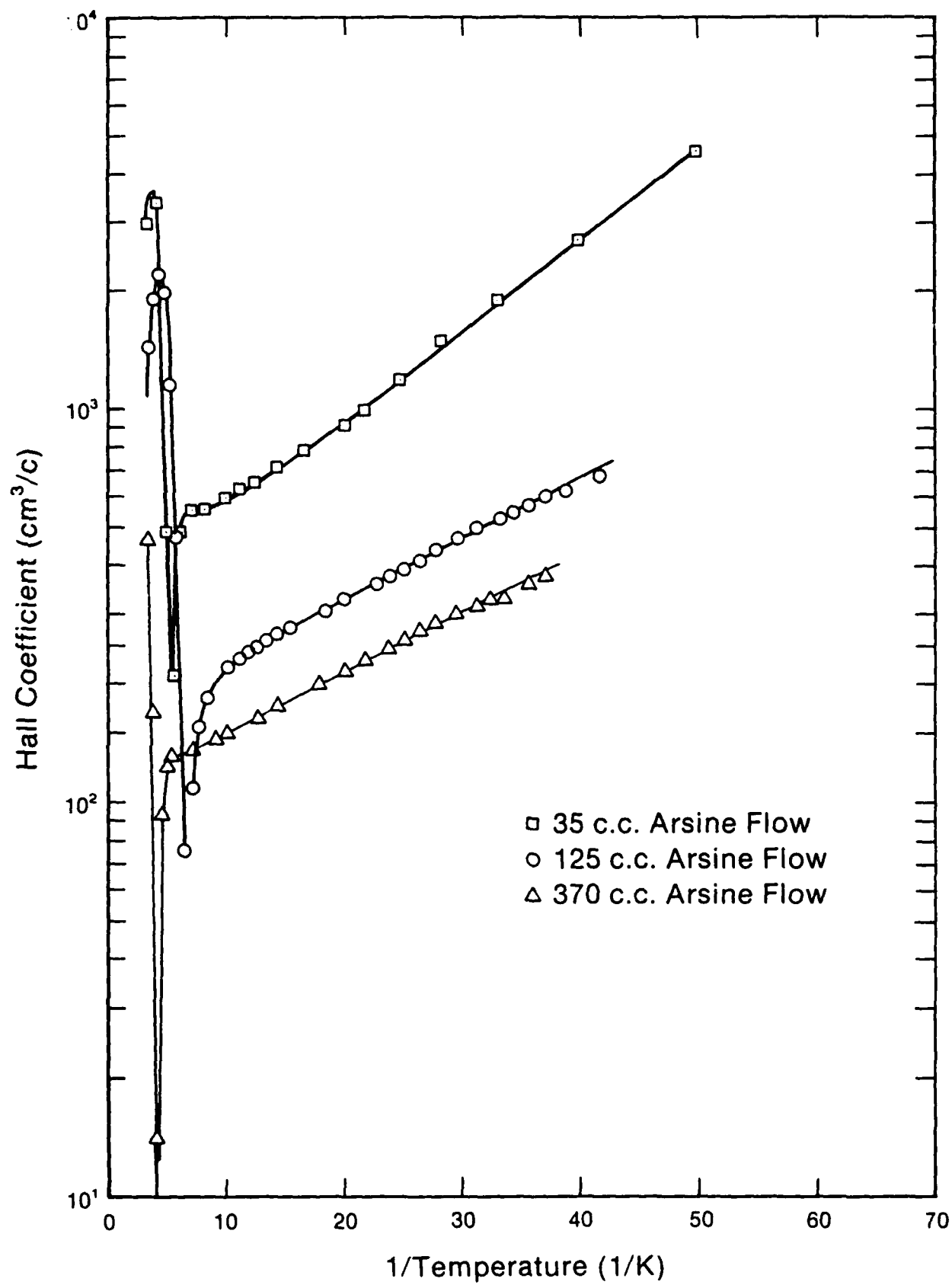


Figure 6. Hall constant vs. arsine flow.

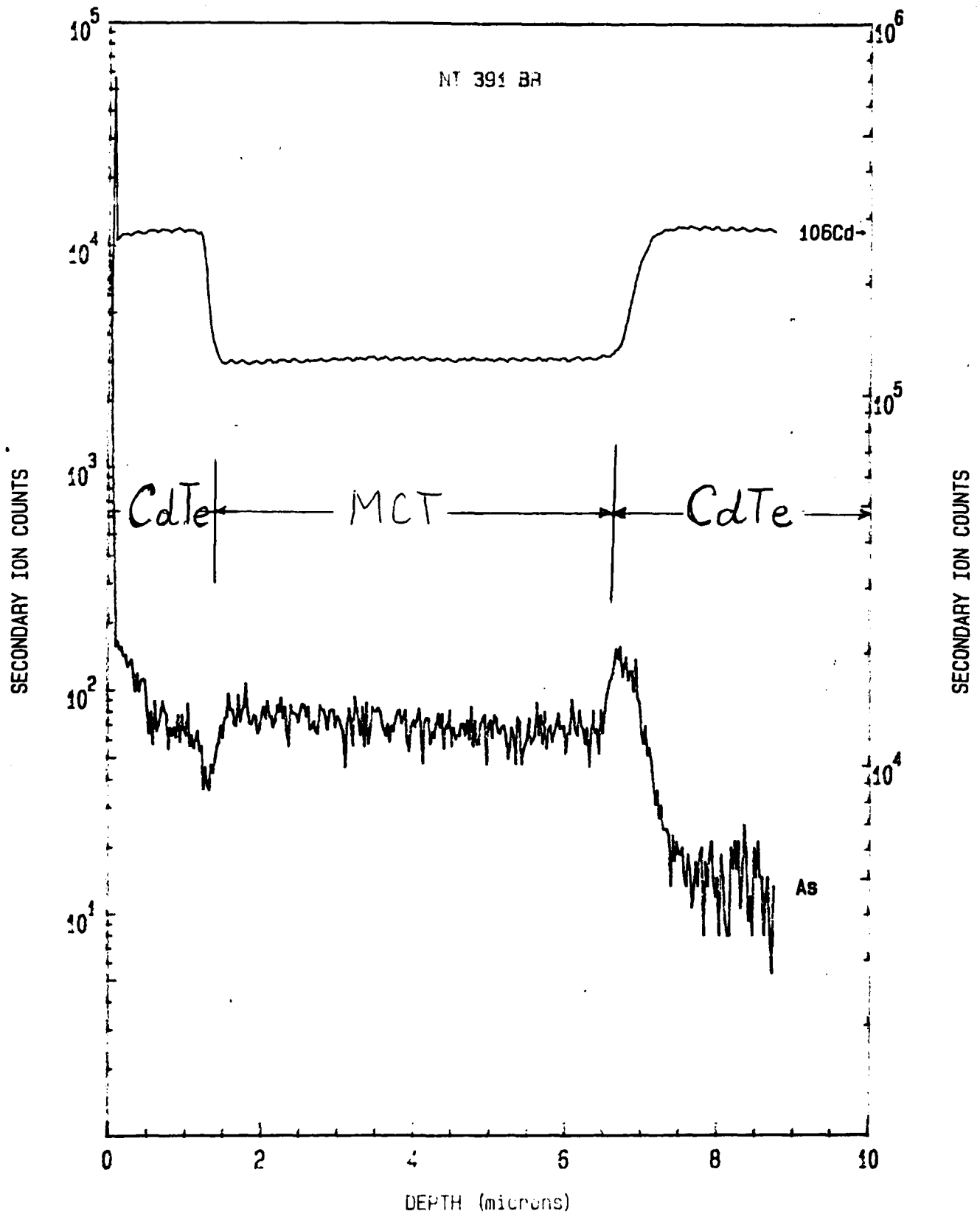


Figure 7. Arsenic signal for a HgCdTe layer with a CdTe cap and a CdTe buffer.

in these doped layers, except for lower doped samples, and at temperatures below 30K. Figure 4 shows the doping concentrations for these layers as a function of arsine flow rate. The linear behavior of this characteristic indicates low compensation to  $3 \times 10^{16} \text{ cm}^{-3}$ . The mobility of these films was in the range of 400-600  $\text{cm}^2/\text{Vs}$ , which is comparable to that of bulk p-type films using Hg-vacancy doping.

In order to determine the acceptor ionization energy and the acceptor doping concentration, the low temperature Hall coefficient curve was fitted to the theoretical model assuming a fully ionized donor  $N_d$ , and a single acceptor  $N_a$  at  $E_a$  above the valence band. The activation energies obtained from this fit are shown in Fig. 5 for a number of layers. The activation energy  $E_a$  was found to decrease with increasing p-doping concentration as expected. Data for the acceptor due to Hg-vacancies is also shown for comparison. Figure 6 shows Hall constant vs.  $1/T$  for three different arsine flow conditions.

P-type doping of these layers due to arsenic incorporation was verified by two definitive experiments. First, pairs of arsenic doped layers were grown, side by side, on CdTe substrates. This was done for a number of samples with doping concentration in the range from  $3 \times 10^{16}/\text{cm}^3$  to  $8.3 \times 10^{16}/\text{cm}^3$ . In each case, one of the samples was annealed for 15 hours at 205°C. Hall measurements were made on annealed as well as unannealed layers. In all cases, the carrier concentration remained the same, confirming that the dopant was thermally stable. A small variation, of about 15% increase in p-doping, was found after annealing. This small increase in the carrier concentration could be due to increased activation of arsenic in HgCdTe, or perhaps due to non-uniformity in doping.

Additionally, we have made SIMS measurements on these layers, courtesy of Dr. G. Scilla of the IBM T.J. Watson Research Center. Figure 7 shows the arsenic signal for one such layer, grown on GaAs with a CdTe cap and a CdTe buffer layer, and again confirms that the p-doping is due to arsenic incorporation.



The composition of the layers was relatively unchanged for doping levels up to  $2 \times 10^{16}/\text{cm}^3$ . Beyond this point, however, the layers became increasingly Hg-rich, with a fall in  $x$ . This may be due to the pre-reaction between dimethylcadmium and arsine, which would reduce the effective partial pressure of dimethylcadmium.

Details of the work described here are the subject of two papers, listed as Appendix B and C at the end of this report.

### 2.5.1 Lifetime Measurements

This is an important aspect of materials characterization, and three approaches are being used by us at the present time. The first of these involves the characterization of photoconductor (PCD) devices, from which the lifetime can be extracted by taking steady state photo-response measurements. This approach requires the fabrication of devices, and is a long, tedious one. Nevertheless, we have made devices suitable for measurement. These devices are mounted in a dewar and illuminated from a black body source with a monochromator and a 50 Hz chopper. Source calibration is done with a TGS secondary standard supplied by the Barnes Engineering Company. The response is measured by means of a lock-in amplifier.

We now present data on a typical sample which has been tested in this manner. For this sample,  $x = 0.266$ ,  $t = 8.0 \mu\text{m}$ , and  $(N_A - N_D) = 4 \times 10^{15}/\text{cm}^3$ . The black body radiation flux was  $1.63 \times 10^{15}$  photons/ $\text{cm}^2/\text{sec}$ , in the  $3 \mu\text{m}$  range. The measured value of sheet conductance was 3300 mho/sq at 77K, resulting in a lifetime of 365 nsec. The calculated theoretical lifetime, assuming Auger and recombination radiation, should be 500 nsec in this case. The lower value obtained on our material is probably due to the fact that the sample surface was not passivated, so that its surface recombination velocity degraded the bulk lifetime to some extent.

A second approach we are also pursuing is the measurement of MOS capacitance

behavior, from which the lifetime can be indirectly determined. This approach is inherently simpler, since it involves less device processing steps than the PCD approach. Using this approach has also resulted in lifetime data comparable to that obtained by the PCD method.

The third approach is an extremely powerful one, which we have recently investigated. This approach, developed by Prof. J.M. Borrego at Rensselaer, consists of measuring the microwave reflectance of a sample under transient illumination.

Figure 8 shows the system we have used. Here, a Gunn diode is used to generate 150 mW of microwave power at  $\sim 36$  GHz. This power is delivered via a hybrid tee to the sample, which is placed on a conductive shorting plane,  $\sim 1$  mm away from the tip of the antenna. The area irradiated by this antenna is approximately  $1 \text{ mm} \times 1 \text{ mm}$ . The reflected signal from the sample is collected by the antenna and detected by a crystal detector. The reflected power is prevented from affecting the load seen by the oscillator by means of an isolator. Thus the oscillator output power remains stable.

The sample is also illuminated locally by an AlGaAs laser, with a spot area of  $0.1 \text{ mm} \times 0.1 \text{ mm}$ . The fall time of this laser is 3 nsec. This limits the lowest lifetime which can be measured by the system.

The induced photoconductivity modulates the microwave power reflected at the sample and this serves as the probe for the excess carrier decay. The reflected microwave signal is detected by a fast responding crystal detector, the output of which is a voltage proportional to the incident microwave power at the detector. The output signal of the detector is proportional to the excess carrier density. The change in reflected microwave power for higher dopings and low lifetimes is small and hence amplification of the signal is required. To obtain a faithful reproduction of the photoconductivity transient a large bandwidth (0.1 to 1300 MHz) a.c. amplifier is used. The transients are viewed on a Tektronix 2432A digital oscilloscope. The bandwidth of the scope is 300 MHz for repetitive

signals. The signal to noise ratio is improved by averaging as many as 256 acquisitions using this scope. The time constant of the decay of the transient reflected microwave power can be shown to be the effective lifetime of carriers in the semiconductor. Figure 9 shows the transient response of a HgCdTe layer with a CdTe cap. Here, 64 measurements were averaged to obtain a signal that is reasonably noise free.

Our early work with this system shows that it is an extremely powerful tool for lifetime measurements, since it is nondestructive, and can be used to probe small regions of a large area sample. Moreover, it can be used for studying the behavior of different surface passivations, as well as for making basic studies of the recombination process.

The system, in its present form, was not designed for use with HgCdTe, and many changes will be required in order to optimize it for this purpose. At the present time it is only capable of being operated at room temperature, so that its adaptation to HgCdTe will necessitate its installation in a cryostat. Additionally, its frequency of operation, 35.5 GHz is not optimum for this semiconductor. Changes here, if made, will be of a major nature.

## 2.6 Characterization

Now that we are routinely growing large area ( $1\text{ cm} \times 1\text{ cm}$ ) HgCdTe material of uniform composition, the characterization effort has become increasingly important. This is because further improvements in material quality are aimed at obtaining improved electronic properties. Here, feedback from the characterization process can be used to provide directions for modification of the growth process.

Currently, a number of characterization tools have been acquired/developed for our work. Fourier Transform IR Spectroscopy continues to be a valuable tool for the measurement of layer thickness and composition. Our instrument, a Mattson Cygnus 100, is computer controlled so that measurements can be made at as many as 100 points over a

1 cm  $\times$  1 cm sample. Both composition and layer thickness can be determined with this instrument. We also use a computer program which we have written to analyze the complex fringe structure which is obtained when HgCdTe films are grown on CdTe/GaAs substrates.

Double crystal x-ray diffraction, using (004) reflections, is routinely used to measure layer quality. Low angle measurements, using (115) reflections, are useful for very thin layers, and also for corroborating strain measurements of HgCdTe films. Computer codes have been written to simulate rocking curves in the presence of strain.

Hall effect measurements are perhaps the most important diagnostic tool for obtaining data on both crystal quality and background concentration. Evaluation of low doped p-type samples is especially difficult, since anomalous results are obtained because of surface inversion effects. Here, it becomes necessary to take Hall data over the 10-300K range, and fit this data to a computer simulation based on the model described in Appendix A. In this manner the effect of the surface can be separated from that of the bulk layer.

### 3. PAPERS AND PRESENTATIONS

We believe that the dissemination of research findings to the scientific community is an important part of a university program such as ours. As a result, a number of papers, based on our work during this year, have been submitted to the professional journals. These are listed, together with their current status. In addition, presentations on this work have been made to DARPA and also at professional society meetings.

#### Publications:

1. W.I. Lee, N.R. Taskar, I.B. Bhat, S.K. Ghandhi and J.M. Borrego, "DLTS Studies of n-CdTe Grown by Organometallic Vapor Phase Epitaxy", Solar Cells, 24, 279 (1988).

2. S.K. Ghandhi, N.R. Taskar, I.B. Bhat, K.K. Parat, D. Terry and H. Ehsani, "Extrinsic p-doped HgCdTe Grown by Organometallic Epitaxy", Appl. Phys. Lett., 53, 1641 (1988).
3. V. Natarajan, N. Taskar, I.B. Bhat and S.K. Ghandhi, "Growth and Properties of  $\text{Hg}_{1-x}\text{Cd}_x\text{Te}$  on GaAs with  $x = 0.27$ ", J. Electron Mater., 17, 479 (1988).
4. N.R. Taskar, I.B. Bhat, K.K. Parat, D. Terry, H. Ehsani and S.K. Ghandhi, "The Organometallic Epitaxy of Extrinsic p-doped HgCdTe", J. Vac. Sci. Tech., A7(2), March/April (1989).

#### Presentations:

1. N.R. Taskar, I.B. Bhat, K.K. Parat, D. Terry and H. Ehsani, "The Organometallic Epitaxy of Extrinsic p-doped HgCdTe", 1988 U.S. Workshop on the Physics and Chemistry of Mercury Cadmium Telluride, Orlando, FL, Oct. 10-12, 1988.
2. I.B. Bhat, H. Ehsani, S. Ghandhi, D. Nucciarone and G. Miller, "The Growth of HgTe and HgCdTe Using Methylallyltelluride", Workshop on Mercury Cadmium Telluride, Washington, DC, Nov. 3, 1988.
3. I. Bhat, H. Ehsani and S. Ghandhi, "Organometallic Vapor Phase Epitaxy of HgTe and HgCdTe Using Methylallyltelluride", 1989 SPIE Conf. on Aerospace Sensing, Orlando, FL, March 27-30, 1989.

#### 4. PLANS FOR THE NEXT YEAR

##### A. Large Area HgCdTe on GaAs

This will be our main focus. Here, there are two issues: uniformity of composition and reduction of hillocks in the grown layers. The new reaction chamber, with adjustments to its parameters, will achieve our uniformity requirements during the next year, so we see no problem here.

The issue of hillocks is a considerably more difficult one. Here, we believe that we can develop techniques for reducing their incidence by at least one to two orders of magnitude.

#### B. Doping of HgCdTe

Our doping studies of p-HgCdTe will be extended to n-type material. Indium will be used as the dopant because of its convenient availability in the form of trimethylindium. If time permits, extrinsic n-p diode structures will also be fabricated.

#### C. Wide Gap Materials

We will begin work on the growth of ZnSe, using a simple reaction chamber borrowed from another system. This will limit our growth of material to small areas; however, we can still acquire useful information about the basic growth process.

#### D. Materials Characterization

Here, a major fraction of our effort will be directed to understanding the annealing behavior of OMVPE grown material. This is a critical issue in the fabrication of structures that are envisioned for this material.

MOS studies of HgCdTe will also be carried out to determine the effect of passivation treatments on HgCdTe. This will also provide information on minority carrier lifetime in our material.

### 5. ANTICIPATED PROBLEMS

No serious problem is anticipated in the area of HgCdTe growth and doping. Characterization, especially that which is focused on the measurement of lifetime, is still a problem because of the need for fabricating structures.

Progress in the growth of ZnSe is critically dependent on the acquisition of PL data on a rapid turn around basis. At the present, we cannot obtain this data on our PL

setup, which will need to be modified to cover the short wavelength region.

Organometallic Vapor Phase Epitaxial Growth of  
HgTe and HgCdTe Using Methylallyltelluride

Ishwara B. Bhat, Hassan Ehsani and Sorab K. Ghandhi

Electrical, Computer and Systems Engineering Department  
Rensselaer Polytechnic Institute  
Troy, New York 12180

### ABSTRACT

HgTe and HgCdTe layers have been grown by organometallic vapor phase epitaxy at low temperature by using methylallyltelluride (MATE), dimethylcadmium (DMCd) and elemental mercury. Use of MATE enabled us to grow layers in the 250-320°C range, which is 50°C lower than the growth temperature when diisopropyltelluride (DIPTe) is used. The layers were characterized by double crystal x-ray diffraction, low temperature Hall measurements and Fourier transform infrared spectroscopy (FTIR). Growth below 340°C resulted in featureless HgTe layers. Layers grown on CdTe are misoriented with respect to the substrate by about 60 to 150 arc-seconds whereas such tilting was not observed when lattice matched CdZnTe substrates were used. The high quality of HgTe grown at low temperature is demonstrated by the very narrow (29 arc seconds) full width at half maximum of the x-ray diffraction curve. HgCdTe layers grown at 320°C showed sharp interference fringes even for thin layers, indicating the presence of a sharp interface.

### 1. INTRODUCTION

There have been recently many reports on the low temperature growth of HgTe and CdTe by organometallic vapor phase epitaxy (OMVPE). Laser or ultra-violet assisted VPE<sup>1</sup>, plasma enhanced VPE<sup>2</sup>, growth by precracking techniques<sup>3</sup> and growth by using less stable Te precursors<sup>4-6</sup> have been reported. Of all these methods, growth by using less stable Te alkyls is the most promising one. Presently, the most common approach is the pyrolysis of using diisopropyltelluride for the Te source<sup>7,8</sup> with a growth temperature around 370°C. Other Te precursors such as ditertiarybutyltelluride<sup>9</sup> and diallyltelluride<sup>10</sup> have been used to grow HgTe or CdTe at low temperature (250-350°C). However, these chemicals have low vapor pressure so that they have to be heated in order to transport sufficient amounts of Te to the reactor. Recently, methylallyltelluride (MATE) has been used to grow HgTe at about 320°C<sup>11</sup>, using dimethylmercury. This Te source has relatively high vapor pressure (6.2 Torr at 20°C) so that it can be transported easily to the reaction zone. None of these new Te precursors have been used to grow HgCdTe layers at the present time. Here, we report on the growth of HgTe and HgCdTe layers using MATE, and the effect of low temperature growth on the quality of the resulting epitaxial layers.

### 2. EXPERIMENTAL

The epitaxial growth of HgTe and HgCdTe was carried out at low pressure (380 Torr) in a vertical reactor using MATE, DMCd and Hg as the Te, Cd and Hg sources respectively. The



substrates were (100) CdTe and (100) CdZnTe, 2 degrees misoriented towards (110). Growth was performed in the temperature range from 250°C to 350°C, with a MAtTe partial pressure of  $1.1 \times 10^{-3}$  atm and an Hg partial pressure of 0.03 atm. The growth rate for HgTe layers was 5  $\mu\text{m/hr}$  at 320°C and 1  $\mu\text{m/hr}$  at 240°C. Double Crystal Rocking (DCR) curves were taken using InSb as the first crystal and Cu  $K_\alpha$  radiation.

### 3. RESULTS AND DISCUSSION

The morphology of an HgTe layer grown at 320°C is shown in Fig. 1. The layer is featureless, without the presence of step features usually observed for growth at higher temperatures using DIPT or DETe. The morphology of a layer grown at 370°C with DIPTe is also shown for comparison. The better morphology of the layer grown with MAtTe is mainly due to the lower temperature growth. Growth at higher temperature using MAtTe resulted in layers with similar step features to those obtained with DIPTe.

The crystal quality of the epilayer was investigated by double crystal x-ray diffraction. Figure 2 shows the DCR curve of the (400) reflection of a 3.4  $\mu\text{m}$  thick HgTe layer grown on a CdTe substrate. The peak separation between the substrate and the epilayer,  $D$ , was found to be a function of the angular position of the sample with respect to the x-ray beam, indicating that the layer is tilted with respect to the substrate. The peak separation  $D$  as a function of rotation angle  $\alpha$  followed the following relationship.

$$D = \Delta\theta + \Delta\phi \cos \alpha$$

Here,  $\Delta\theta$  is the peak separation caused by lattice mismatch in the growth direction and  $\Delta\phi$  corresponds to the epilayer misorientation with respect to the substrate. This is illustrated in Fig. 3. The epilayer is seen to be tilted an additional 60 arc-seconds from the surface normal. Epilayer tilts of this type have been observed in many other lattice mismatched systems<sup>12-14</sup>. The lattice tilt was observed in layers grown at lower temperature, but generally not seen when layers were grown at higher temperature using DIPTe or DETe. It is probable that growth at higher temperature results in significant interdiffusion between the HgTe and CdTe substrate. This causes a gradual change of the lattice constant from that of CdTe to HgTe, so that no tilt of the epilayer is observed. From the value of  $\Delta\theta$ , the lattice constant in the growth direction was determined as a function of epilayer thickness, and is shown in Fig. 4. This lattice constant reaches its relaxed, bulk value beyond about 4  $\mu\text{m}$ .

It is interesting to note that the measured lattice constant of HgTe does not reach the bulk value even for a 3.5  $\mu\text{m}$  thick layer. This shows that a significant amount of strain is still present on such a thick HgTe layer. On the other hand, in many other systems, such as ZnSe on GaAs<sup>12</sup>, or GaInAs on GaAs<sup>15</sup>, the lattice constant of the epilayer reaches the bulk value within about 1  $\mu\text{m}$ . Similarly, when CdTe is grown on GaAs<sup>16</sup>, beyond about 1  $\mu\text{m}$ , the CdTe layer is found to be strain free.

The FWHM of the x-ray diffraction curve of the epilayer is shown in Fig. 5 as a function of layer thickness. The effect of interface dislocations on the FWHM is clearly seen from the monotonic decrease of x-ray FWHM as the thickness is increased. Assuming that the line broadening is due to the presence of dislocations only, we can calculate the dislocation density given by  $f/9b^2$ , where  $f$  is the FWHM and  $b$  is the Burgers vector, which for the zincblende structure is  $a/2$  ( $a$

is the lattice constant)<sup>17</sup>. A FWHM of 200 arc-seconds corresponds to a dislocation density of  $4 \times 10^8 \text{ cm}^{-2}$ . From the lattice mismatch, we can estimate the misfit dislocation density to be  $2.6 \times 10^9 \text{ cm}^{-2}$ , which is on the same order as that obtained from the x-ray curve data.

With CdZnTe substrates, which are more closely lattice matched to the HgTe layer, different results were obtained. Figure 6 shows the DCR curve for a 1.7  $\mu\text{m}$  thick HgTe layer grown on a CdZnTe substrate. Both the epilayer and the substrate have almost identical x-ray FWHM values (29 versus 28 arc-seconds), indicating the excellent quality of the epilayer that could be obtained by the low temperature process. The lattice mismatch between the substrate and the layer is estimated to be below 0.07%, assuming that the epilayer is pseudomorphic. The layer followed the orientation of the substrate, whereas, a small amount (60-150 arc-sec.) of layer tilt with respect to the substrate was observed when CdTe substrates were used. All the layers grown on CdZnTe substrates had FWHM values in the range 28 to 40 arc-seconds, closely replicating the substrate quality. This illustrates the importance of lattice matching on the quality of the layers.

MCT layers were grown at 320°C, for the first time, using MATe by adding DMCD. Figure 7 shows the Fourier transform infrared spectrum (FTIR) for a layer grown on a CdTe substrate. Excellent epilayer substrate interface is demonstrated by the sharp fringes present, even when the layer is only 1.7  $\mu\text{m}$  thick. For layers grown with DIPTe at higher temperature, these fringes were less sharp due to the interdiffusion effects.

#### 4. CONCLUSION

We have successfully used MATe to grow excellent quality HgTe layers on CdZnTe substrates. When the layers were grown on CdTe substrates, they grow with a tilt (50 to 150 arc-seconds) with respect to the substrates. In addition, the epilayers were tetragonally distorted up to a thickness of at least 4  $\mu\text{m}$ . Layers grow without any tilt when CdZnTe substrates, which are better lattice matched than CdTe substrates, are used. The FWHM of the x-ray diffraction peak of these layers were in the range of 28 to 40 arc-seconds. MCT layers grown with this chemical at a low temperature exhibits sharp interference fringes indicating the presence of sharp interface between MCT and CdTe substrates.

#### 5. ACKNOWLEDGEMENT

The authors would like to thank J. Barthel for technical assistance on this program and P. Magilligan for manuscript preparation. We would like to thank Dr. G. Miller of the American Cyanamid Corporation for providing the MATe and C.J. Johnson and S. McDevitt of II-VI Inc. for providing the CdZnTe substrates. This work was sponsored by the Defense Advanced Research Projects Agency (contract No. N-00014-85-K-0151), administered through the Office of Naval Research, Arlington, VA. This support is greatly appreciated.

#### 6. REFERENCES

1. S.J.C. Irvine, CRC Critical Reviews in Solid State and Materials Science, Vol. 13, 279 (1987).
2. L.M. Williams, P.Y. Lu, C.H. Wang, J.M. Parsey and S.N.G. Chu, Appl. Phys. Lett., 51, 1738 (1987).

3. L.M. Williams, P.Y. Lu, S.N.G. Chu and C.H. Wang, J. Appl. Phys., 62, 295 (1987).
4. L.S. Lichtmann, J.D. Parsons and E.H. Cirlin, J. Cryst. Growth, 86, 217 (1988).
5. D.W. Kisker, M.L. Steigerwald, T.Y. Kometani and K.S. Jeffers, Appl. Phys. Lett., 50, 1681 (1987).
6. W.E. Hoke and P.J. Lemonias, Appl. Phys. Lett., 46, 398 (1985).
7. I.B. Bhat and S.K. Ghandhi, J. Cryst. Growth, 75, 241 (1986).
8. I.B. Bhat, H. Fardi and S.K. Ghandhi, J. Vac. Sci. Technol., A6, 2800 (1988).
9. W.E. Hoke and P.J. Lemonias, Appl. Phys. Lett., 48, 1669 (1986).
10. R. Korenstein, W.E. Hoke, P.J. Lemonias, K.T. Higa and D.C. Harris, J. Appl. Phys., 62, 4929 (1987).
11. J.D. Parsons and L.S. Lichtmann, J. Cryst. Growth, 86, 222 (1988).
12. A. Ohki, N. Shibata and S. Zembutsu, J. Appl. Phys., 64, 694 (1988).
13. H. Nagai, J. Appl. Phys., 45, 3789 (1974).
14. I.B. Bhat, K. Patel, N.R. Taskar, J.E. Ayers and S.K. Ghandhi, J. Vac. Sci. Technol., 88, 23 (1988).
15. P.J. Orders and B.F. Usher, Appl. Phys. Lett., 50, 980 (1987).
16. D.J. Olego, J. Petruzzello, S.K. Ghandhi, N.R. Taskar and I.B. Bhat, Appl. Phys. Lett., 51, 129 (1987).
17. H. Shtrikman, A. Raizman, M. Oron and D. Eger, J. Cryst. Growth, 88, 522 (1988).

# Extrinsic *p*-type doping of HgCdTe grown by organometallic epitaxy

S. K. Ghandhi, N. R. Taskar, K. K. Parat, D. Terry, and I. B. Bhat

Electrical, Computer, and Systems Engineering Department, Rensselaer Polytechnic Institute, Troy, New York 12180

(Received 17 May 1988; accepted for publication 17 August 1988)

In this letter, we report on the extrinsic *p*-type doping of mercury cadmium telluride (MCT), during growth by organometallic vapor phase epitaxy. Arsine gas in hydrogen was used as the dopant source. The layers were characterized by Hall effect and by resistivity measurements over the temperature range from 20 to 300 K. The acceptor ionization energy was obtained for different doping concentrations from the Hall coefficient data. Its value decreases with doping concentration, and is about 8.5 meV for a doping of  $1.1 \times 10^{16} \text{ cm}^{-3}$ . This is a factor of 2 lower than the ionization energy of mercury vacancies, for layers of this (27–30% cadmium) composition and doping level. Annealing at 205 °C for 15 h in a Hg-rich ambient did not produce significant changes in the measured doping concentration. This indicates that the acceptor level is extrinsic in nature, and that arsenic behaves as a stable acceptor dopant in MCT, grown by organometallic epitaxy.

Mercury cadmium telluride (MCT or  $\text{Hg}_{1-x}\text{Cd}_x\text{Te}$ ) layers, grown by organometallic vapor phase epitaxy (OMVPE), have shown considerable promise for use in far-infrared detector applications in recent years.<sup>1–5</sup> Layers with uniformity in composition and thickness that are required for present day device structures can be grown by this method.<sup>6,7</sup> The as-grown material is generally *p* type due to the presence of native defects such as mercury vacancies, provided that the residual (donor) impurities in the starting chemicals are in very low concentration. In order to obtain layers with stable and controllable doping, either *n* or *p* type, it is necessary to introduce external impurities. Both group V elements, which are incorporated on the Te sublattice, and the group I elements, which incorporate on the metal sublattice, act as *p*-type dopants.<sup>8</sup> Group V elements are preferred because they are much slower diffusing acceptors and hence can be used to form stable device structures.<sup>9</sup> However, doping of MCT by group V elements such as Sb, As, and P has not been very successful by many growth methods. For example, As and Sb doping by liquid phase epitaxy (LPE) from Te-rich solutions does not always result in *p*-type layers, even after the Hg vacancy concentration is reduced by low-temperature annealing in Hg-rich ambients.<sup>10</sup> In molecular beam epitaxy, both Sb and As behave as *n*-type dopants.<sup>11</sup>

In this letter, we report on the successful *p* doping of HgCdTe, grown by OMVPE using arsine gas as the dopant source. In previous work,<sup>12</sup> we have shown that this dopant can be used successfully to obtain *p*-type doping of CdTe epilayers.

MCT layers were grown in an atmospheric pressure, horizontal reactor using diisopropyl telluride, dimethylcadmium, and elemental mercury. The alloy growth method was used in which Cd, Te, and Hg sources are introduced simultaneously into the reactor. Substrates were 2° misoriented (100), semi-insulating GaAs, on which a 2-μm-thick undoped CdTe buffer layer was first grown at 350 °C. In previous studies,<sup>13</sup> we have shown that this thickness is sufficient so that subsequent MCT layers are comparable in quality to those grown on bulk CdTe. A 0.5-μm-thick CdTe cap

was grown on the MCT as a passivant layer. The thickness of all the MCT layers in this study was 7 μm, and the composition *x* was in the range 0.27–0.31.

Hall mobility and resistivity measurements were made in cloverleaf-patterned samples with a magnetic field strength of 2.1 kG, and over the temperature range from 20 to 300 K. Measurement over this temperature range is necessary for *p*-type layers, in order to determine the presence of any surface inversion.<sup>14</sup> Only layers which showed negligible surface inversion at low temperatures were used in our study. Ohmic contacts were made by etching the CdTe cap near the contact area and evaporating Au onto MCT. Some difficulty was encountered in making contacts which were suitable over the full temperature range.

All the layers grown in this reactor, without any intentional doping, were weakly *n*-type (in the low  $10^{15} \text{ cm}^{-3}$  range) due to the presence of residual impurities in the chemicals. The Hall coefficient and Hall mobility for a MCT layer with no intentional doping is shown in Fig. 1. The curve shows typical *n*-type behavior with a carrier concentration of  $3.5 \times 10^{15} \text{ cm}^{-3}$ . The Hall mobility at 40 K was  $2.3 \times 10^4 \text{ cm}^2/\text{V s}$ , which is typical for layers of this composition (30% Cd) and doping concentration. This result shows that the net Hg vacancy concentration in the layers is low, assuming low compensation. The *n*-type doping levels generally observed were in the range  $2\text{--}4 \times 10^{15} \text{ cm}^{-3}$ , for layers of 20–30% cadmium composition.

Arsenic-doped layers were grown with *p*-doping levels from  $3.5 \times 10^{15}$  to  $1.1 \times 10^{16} \text{ cm}^{-3}$ . No evidence of surface inversion was observed in these doped layers, except for lower doped samples, and at temperatures below 30 K. Figure 2 shows the Hall coefficient as a function of inverse temperature for a MCT layer with *x* = 0.27 grown with 350 sccm of arsine flow, with a doping concentration of about  $1.1 \times 10^{16} \text{ cm}^{-3}$ . Here, classical *p*-type behavior is observed throughout the temperature range. Figure 3 showed the measured mobility as a function of temperature for this layer. The low-temperature mobility values remained constant at  $\sim 500 \text{ cm}^2/\text{V s}$  down to 20 K and showed negligible change ( $< 5\%$ ) when the magnetic field was increased from 2.1 to

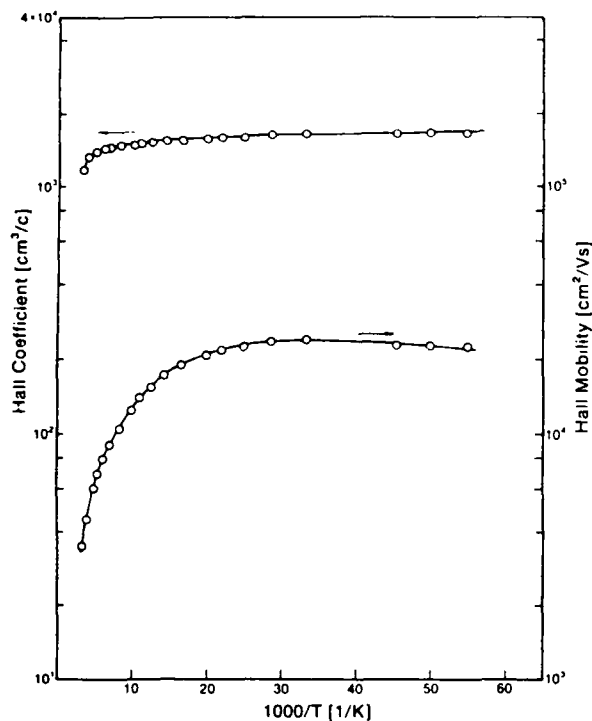


FIG. 1. Hall coefficient and Hall mobility as a function of reciprocal temperature for an undoped MCT layer of composition  $x = 0.3$ .

4.5 kG, indicating the absence of any surface inversion. The high value of hole mobility observed here indicates that most of the As is electrically active in the layer.

The doping concentration increased from  $3.5 \times 10^{15}$  to

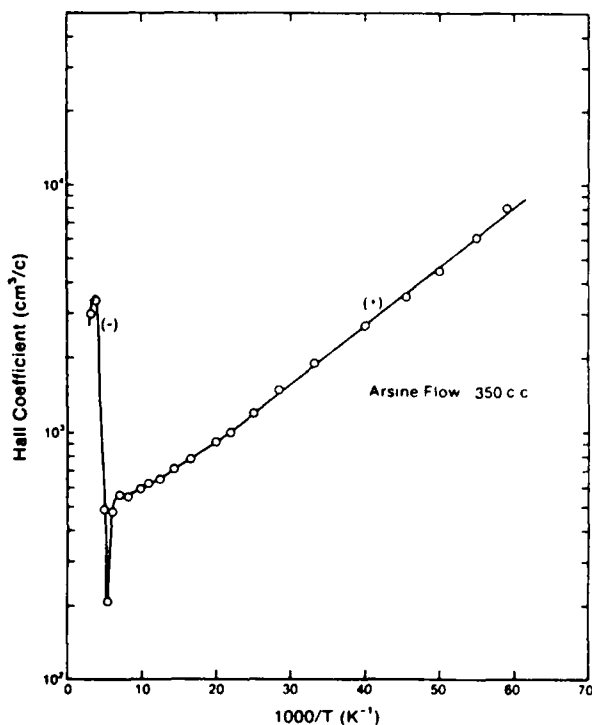


FIG. 2. Hall coefficient as a function of reciprocal temperature for a MCT layer, grown with an arsine flow of 350 sccm/min ( $1.7 \times 10^{-4}$  atm).

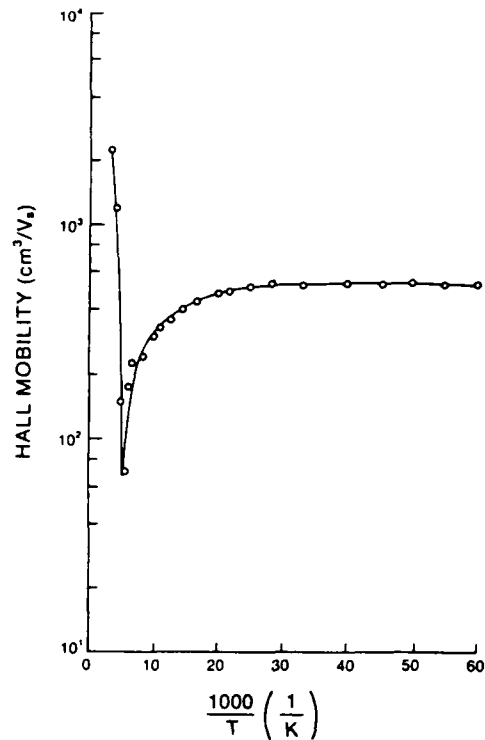


FIG. 3. Hall mobility as a function of reciprocal temperature for the layer in Fig. 2.

$1.1 \times 10^{16} \text{ cm}^{-3}$  as the arsine flow was increased from 60 to 350 sccm, with all other growth parameters held constant. An almost linear relationship between the doping concentration and the arsine flow rate was observed. This suggests a high degree of As incorporation into the Te lattice sites, and indicates the possibility of increasing the doping concentration beyond  $1.1 \times 10^{16} \text{ cm}^{-3}$ . Finally, all the layers studied showed high mobility (400–600  $\text{cm}^2/\text{V s}$ ) at low temperature.

In order to determine the acceptor ionization energy

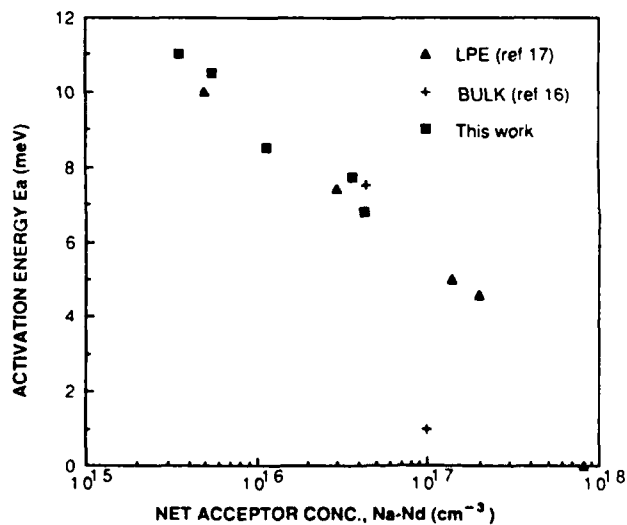


FIG. 4. Activation energy of As acceptors as a function of the net acceptor concentration,  $N_a - N_d$ .

and the acceptor doping concentration, the low-temperature Hall coefficient curve was fitted to the theoretical model assuming a fully ionized donor  $N_d$  and a single acceptor  $N_a$  at  $E_a$  above the valence band.<sup>14,15</sup> The activation energies obtained from this fit are shown in Fig. 4. Also shown are the ionization energies measured for arsenic in doped bulk wafers<sup>16</sup> and in LPE epilayers grown from Hg-rich melts,<sup>17</sup> for  $x$  values in the range 0.2–0.3. The activation energy  $E_a$  decreased with increasing doping concentration as expected, due to the increased interaction between neighboring impurity atoms.<sup>17,18</sup> The ionization energy for the mercury acceptor is generally found to be a factor of 2 higher than that for the arsenic.

Isothermal annealing was carried out in order to annihilate the excess mercury vacancies, and reduce their contribution to the measured acceptor concentration. The annealing was performed for 15 h at 205 °C, in a sealed quartz ampoule in which a small amount of Hg was placed to maintain a mercury-rich ambient. This temperature should be more than sufficient to convert the whole of the layer to  $n$  type,<sup>19</sup> if the  $p$  doping observed is due to the mercury vacancies alone. For these experiments, uncapped, doped MCT layers were grown side by side, in the same run. CdTe substrates were used in order to eliminate the possibility of any influence from the GaAs substrate during the annealing step. The as-grown layer had a  $p$ -type carrier concentration of  $3.7 \times 10^{16} \text{ cm}^{-3}$ . The second layer, annealed in a Hg-rich ambient as described above, had a measured carrier concentration of  $4.3 \times 10^{16} \text{ cm}^{-3}$ . The small increase observed here was most probably due to the nonuniformity in the doping of the adjacent layers. However, increased activation of As cannot be ruled out, even though such activation of  $p$  dopants has not been observed in low-temperature annealed layers grown by LPE.<sup>10</sup> In either case, it is seen that the use of arsine gas results in a controllable  $p$  doping which can be relatively stable during low-temperature processing. The Hall constant curves for these samples are shown in Fig. 5.

In conclusion, we have shown that As can be incorporated in MCT, grown by OMVPE, using arsine in hydrogen as the dopant gas. Layers were grown with carrier concentration in the range  $3.5 \times 10^{15}$ – $3.7 \times 10^{16} \text{ cm}^{-3}$ , and higher doping concentrations could be achievable by using a higher concentration of arsine in hydrogen. All the layers studied showed freezeout at low temperature, and the ionization energy was calculated from the theoretical fit to the Hall coefficient curve as a function of temperature. The  $E_a$  value decreased with increasing doping concentration, and is about 8.5 meV for a doping level of  $1.1 \times 10^{16} \text{ cm}^{-3}$ . Isothermal annealing of doped layers in Hg, at 205 °C for 15 h, did not decrease the acceptor doping concentration, confirming that the doping observed is due to arsenic, and not to an excess of Hg vacancies. Thus, extrinsic  $p$  doping of MCT has been demonstrated by this growth technique.

The authors would like to thank J. Barthel for technical assistance on this program and P. Magilligan for manuscript preparation. This work was sponsored by the Defense Advanced Research Projects Agency (contract No. N-00014-

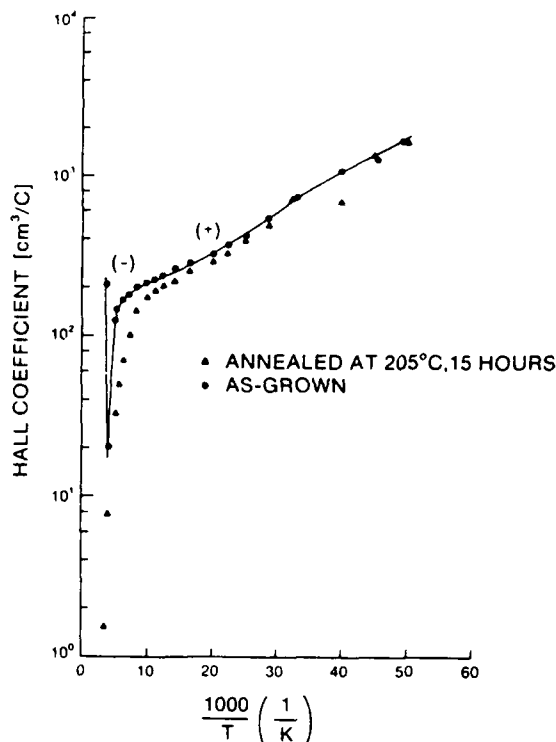


FIG. 5. Hall coefficient as a function of reciprocal temperature for an as-grown and an annealed MCT layer doped with As. The Cd composition of both the layers was  $\sim 0.31$ .

85-K-0151), administered through the Office of Naval Research, Arlington, VA. This support is greatly appreciated.

<sup>1</sup>S. J. Irvine and J. B. Mullin, *J. Cryst. Growth* **55**, 107 (1981).

<sup>2</sup>S. K. Ghandhi and I. B. Bhat, *Appl. Phys. Lett.* **44**, 779 (1984).

<sup>3</sup>W. E. Hoke, P. J. Lemonias, and R. Taczewski, *Appl. Phys. Lett.* **45**, 1092 (1984).

<sup>4</sup>J. L. Schmit, *J. Vac. Sci. Technol. A* **3**, 89 (1985).

<sup>5</sup>W. E. Hoke and P. J. Lemonias, *Appl. Phys. Lett.* **48**, 1669 (1986).

<sup>6</sup>S. K. Ghandhi, I. B. Bhat, and H. Fardi, *Appl. Phys. Lett.* **52**, 392 (1988).

<sup>7</sup>J. Thompson, P. Mackett, L. M. Smith, D. J. Cole-Hamilton, and D. V. Shenai-Khatkhate, *J. Cryst. Growth* **86**, 233 (1988).

<sup>8</sup>P. Capper, *J. Cryst. Growth* **57**, 280 (1982).

<sup>9</sup>M. Brown and A. F. W. Willoughby, *J. Cryst. Growth* **59**, 27 (1982).

<sup>10</sup>H. R. Vydyanath, J. A. Ellsworth, and C. M. Devaney, *J. Electron. Mater.* **16**, 13 (1987).

<sup>11</sup>P. S. Wijewarnasuriya, I. K. Sou, Y. J. Kim, K. K. Mahavadi, S. Sivananthan, M. Bourkerche, and J. P. Faurie, *Appl. Phys. Lett.* **51**, 2025 (1987).

<sup>12</sup>N. R. Taskar, V. Natarajan, I. B. Bhat, and S. K. Ghandhi, *J. Cryst. Growth* **86**, 228 (1988).

<sup>13</sup>I. B. Bhat, N. R. Taskar, and S. K. Ghandhi, *J. Vac. Sci. Technol. A* **4**, 2230 (1986).

<sup>14</sup>L. F. Lou and W. H. Frye, *J. Appl. Phys.* **56**, 2253 (1984).

<sup>15</sup>C. T. Elliott, I. Melngailis, T. C. Herman, and A. G. Foyt, *J. Phys. Chem. Solids* **33**, 1527 (1972).

<sup>16</sup>P. Capper, J. J. G. Gosney, C. L. Jones, I. Kenworthy, and J. A. Roberts, *J. Cryst. Growth* **71**, 57 (1985).

<sup>17</sup>M. H. Kalisher, *J. Cryst. Growth* **70**, 365 (1984).

<sup>18</sup>P. P. Debye and E. M. Conwell, *Phys. Rev.* **93**, 693 (1954).

<sup>19</sup>C. L. Jones, M. J. T. Queich, P. Capper, and J. J. G. Gosney, *J. Appl. Phys.* **53**, 9080 (1982).

# APPENDIX - C

## THE ORGANOMETALLIC EPITAXY OF EXTRINSIC p-DOPED HgCdTe

by

N.R. Taskar

I.B. Bhat

K.K. Parat

D. Terry

H. Ehsani

and

S.K. Ghandhi

Electrical, Computer, and Systems Engineering Department

Rensselaer Polytechnic Institute

Troy, New York 12180

SK-88.43

October 24, 1988

## ABSTRACT

Extrinsic p-doped mercury cadmium (MCT) layers have been grown by organometallic vapor phase epitaxy, using arsine in hydrogen as the dopant gas. Controllable doping in the range  $3.5 \times 10^{15}$  to  $4.3 \times 10^{16}$  was obtained when grown on GaAs with CdTe buffer layers. Consistently higher doping concentration (a factor of 2-4) was observed when a CdTe substrate was used. This is believed to be due to higher dislocation densities present when grown on GaAs, around which As may segregate. The cadmium fraction fell at very high arsine flow; we believe that this is due to the pre-reaction of dimethylcadmium with arsine. Isothermal annealing under a Hg-rich ambient of MCT grown on CdTe substrates did not produce significant changes in the measured doping concentration. This indicates that the acceptor level is extrinsic in nature and that arsenic behaves as a stable acceptor dopant in MCT. The activation energy of this acceptor was determined as a function of doping, and is about one half the value of the acceptor due to the Hg-vacancies.



## INTRODUCTION

Mercury cadmium telluride (MCT or  $\text{Hg}_{1-x}\text{Cd}_x\text{Te}$ ) layers, grown by organometallic vapor phase epitaxy (OMVPE), have shown considerable promise for use in far infrared detector applications in recent years<sup>1-5</sup>. Layers with the uniformity in composition and thickness that are required for present day device structures can be grown by this method<sup>6,7</sup>. The as-grown material is generally p-type due to the presence of native defects such as mercury vacancies, provided that the residual (donor) impurities in the starting chemicals is in very low concentration. To obtain n-type material, these layers are often annealed at low temperature under a Hg-rich ambient. Instead of relying on stoichiometry control, it is desirable to introduce external impurities during growth to get n- or p-type layers. The doping levels of such layers are potentially more stable during subsequent device processing than those obtained by native defects.

Various impurities have been used in bulk and many epitaxial growth methods<sup>8</sup>. Elements from group III and group VII behave as n-type dopants and elements from group I and group V act as p-type. For p-doping, group V elements are preferred because they are much slower diffusing acceptors and hence can be used to form stable device structures<sup>9</sup>. However, doping of MCT by group V elements such as Sb, As and P has not been very successful by many growth methods. For example, As and Sb doping by liquid phase epitaxy (LPE) from Te-rich solutions does not always result in p-type layers, even after the Hg vacancy concentration is reduced by low temperature anneal in Hg-rich ambients<sup>10</sup>. In molecular beam epitaxy, both Sb and As behave as n-type dopants<sup>11</sup>.

This paper describes the study of acceptor doping of MCT layers, grown by OMVPE, using arsine gas as the dopant source. In an earlier study<sup>12</sup>, we have shown that this dopant can be used successfully to obtain p-type doped CdTe layers.

## EXPERIMENTAL

MCT layers were grown in an atmospheric pressure, horizontal reactor using diisopropyl telluride, dimethylcadmium and elemental mercury. The alloy growth method was used in which Cd, Te and Hg sources are introduced simultaneously into the reactor. Substrates were 2° misoriented (100), semi-insulating GaAs, on which a 2  $\mu\text{m}$  thick undoped CdTe buffer layer was first grown at 350°C. In previous studies<sup>13</sup>, we have shown that this thickness is sufficient so that subsequent MCT layers are comparable in quality to those grown on bulk CdTe. A 0.5  $\mu\text{m}$  thick CdTe cap was grown on the MCT as a passivant layer. The thickness of all the MCT layers reported here was 7  $\mu\text{m}$ , and the composition  $x$  was in the range 0.27 to 0.31. For doping of MCT layers, we have used 50 and 500 parts per million arsine in hydrogen. All the flows mentioned in this paper are in terms of 500 ppm AsH<sub>3</sub> in H<sub>2</sub>, for the sake of clarity.

Hall mobility and resistivity measurements were made in cloverleaf-patterned samples with a magnetic field strength of 2.1 kG, and over the temperature range from 20 to 300K. Measurement over this temperature is necessary for p-type layers, in order to determine the presence of any surface inversion<sup>14</sup>. Only layers which showed negligible surface inversion at low temperatures were used in our study. Ohmic contacts were made by etching the CdTe cap near the contact area and evaporating Au on to the MCT. The CdTe cap is always present in the active area, which enabled us to measure low doped p-type layers without seeing surface inversion effects down to 30K.

## RESULTS AND DISCUSSION

Many undoped layers were grown on GaAs in this reactor, in order to determine the background doping level. This was necessary in order to separate out the doping effect due to Hg vacancies from that of the intentional dopant, As. All the layers grown in this reactor, without any intentional doping, were weakly n-type (in the low  $10^{15} \text{ cm}^{-3}$

range) or weakly p-type with anomalous behavior. This background doping level (either n-type or p-type) seems to depend on many factors such as type of substrates used (CdTe or GaAs), the reactor configuration, the Hg partial pressure and the purity of the chemicals. In all the growth runs, all these parameters were kept constant so that any changes in the doping concentration measured are due to arsine alone. Figure 1 shows the Hall mobility and Hall coefficient for a typical undoped MCT layer grown on GaAs with a CdTe buffer layer. The curve shows n-type behavior with a carrier concentration of  $3.5 \times 10^{15} \text{ cm}^{-3}$ . The Hall mobility at 40K was  $2.3 \times 10^4 \text{ cm}^2/\text{Vs}$ , which is typical for layers of this composition (30% Cd) and doping concentration. This result shows that the net Hg vacancy concentration in the layers is low, assuming low compensation.

Arsenic doped MCT layers on GaAs were grown with p-doping levels in the range  $3.5 \times 10^{15} \text{ cm}^{-3}$  to  $4.3 \times 10^{16} \text{ cm}^{-3}$ . No evidence of surface inversion was observed in these doped layers, except for lower doped samples, and at temperatures below 30K. Figure 2 shows the Hall coefficient versus inverse temperature for three layers grown with different flows of  $\text{AsH}_3$ . For all layers, the composition  $x$  was in the range 0.27 to 0.3. It is clear that an increase in doping concentration is observed as the  $\text{AsH}_3$  flow is increased. For a 50 sccm of  $\text{AsH}_3$  flow, the carrier concentration measured was  $1.5 \times 10^{16} \text{ cm}^{-3}$  and for a 350 sccm of  $\text{AsH}_3$  flow, the carrier concentration was  $4.3 \times 10^{16} \text{ cm}^{-3}$ . As expected, the transition temperature, from n- to p-type, occurs at higher temperature for higher doped layers. Preliminary studies done with layers of various composition indicates that the doping level is rather insensitive to composition.

Figure 3 shows the net acceptor concentration as a function of arsine flow rate. The measured doping concentration increased from  $3.5 \times 10^{16} \text{ cm}^{-3}$  to  $4.3 \times 10^{16} \text{ cm}^{-3}$  as the arsine flow was increased from 5 sccm to 250 sccm, with all the other parameters held constant. The mobility of these films was in the range of 400-600  $\text{cm}^2/\text{Vs}$ , which is comparable to that of bulk p-type films using Hg-vacancy doping. Increasing the arsine

flow beyond 250 sccm did not increase the doping, but such films had lower temperature mobilities compared to those grown with 250 sccm arsine flow. This indicates that these films are more compensated.

We have seen consistently higher doping when a CdTe substrate is used instead of a GaAs substrate, by a factor of 2-4. The maximum acceptor concentration obtained when grown on CdTe substrates was  $8.3 \times 10^{16} \text{ cm}^{-3}$ . Similar substrate effects were noted when arsine gas was used to dope CdTe layers, i.e., epitaxial CdTe grown on CdTe had higher active concentration than CdTe grown on GaAs. We believe this is due to the difference in the crystal quality between the layers grown on these two substrates. The MCT layers grown on GaAs may have higher densities of dislocations, around which As may segregate, thus showing a lower acceptor concentration.

The composition of the layers was also a function of arsine flow at high doping levels. The layer became increasingly Hg-rich and composition  $x$  fell below 0.2 as the arsine flow was increased beyond 350 sccm. This may be because of the pre-reaction between dimethylcadmium and arsine, which would reduce the effective partial pressure of dimethylcadmium. Changes in the layer composition with dopant gas were also observed by other workers in OMVPE-IMP grown layers<sup>15</sup> doped with trimethylarsenic (TMAs) and trimethylantimony (TMSb). They have seen an increase in  $x$  when TMAs was added, whereas a decrease in  $x$  was observed when TMSb was introduced. It appears the introduction of these dopants alters the relative adsorption of Cd and Hg species, thus changing the composition of the grown layers.

In order to determine the acceptor ionization energy and the acceptor doping concentration, the low temperature Hall coefficient curve was fitted to the theoretical model assuming a fully ionized donor  $N_d$ , and a single acceptor  $N_a$  at  $E_a$  above the valence band<sup>14,16</sup>. The activation energies obtained from this fit are shown in Fig. 4. The activation energy  $E_a$  decreased with increasing doping concentration as expected, due to the

increased interaction between neighboring impurity atoms<sup>18,19</sup>. The figure also shows the ionization energy for the Hg-vacancy acceptor, obtained from Ref (17). The ionization energy obtained for arsenic is consistently a factor of 2 less than that for Hg acceptors. The same order of difference in the ionization energy between Hg vacancies and external impurities has been observed in bulk and LPE doped films.

Isothermal annealing was carried out in order to annihilate the excess mercury vacancies, and reduce their contribution to the measured acceptor concentration. The annealing was performed for 15 hours at 205°C, in a sealed quartz ampoule in which a small amount of Hg was placed to maintain a mercury-rich ambient. This temperature should be more than sufficient to convert the whole of the layer to n-type<sup>20</sup>, if the p-doping observed is due to the mercury vacancies alone. For these experiments, uncapped, doped MCT layers were grown side-by-side, in the same run. CdTe substrates were used in order to eliminate the possibility of any influence from the GaAs substrate during the annealing step. Several layers, with the doping concentrations in the range  $3 \times 10^{16} \text{ cm}^{-3}$  to  $8.3 \times 10^{16} \text{ cm}^{-3}$  were annealed. In all cases, there was no measurable change in the doping concentration. Both annealed and unannealed layers had the carrier concentration within 15%. Figure 5 shows the Hall coefficient vs. temperature for one such layer where the as-grown layer had the carrier concentration of  $3.7 \times 10^{16} \text{ cm}^{-3}$ . The carrier concentration after annealing was  $4.3 \times 10^{16} \text{ cm}^{-3}$ . This small increase in the carrier concentration could be due to increased activation of arsenic in MCT, or perhaps due to non-uniformity in doping. A layer with carrier concentration of  $8.3 \times 10^{16}$  also remained relatively unchanged after annealing.

## CONCLUSIONS

We have shown that As can be incorporated in MCT, grown by OMVPE using arsine as the dopant gas. Layers were grown with carrier concentration in the range

$3.5 \times 10^{15} \text{ cm}^{-3}$  to  $8.3 \times 10^{16} \text{ cm}^{-3}$ . All the layers showed the freezeout at lower temperature and the ionization energy was calculated from a theoretical fit to the Hall coefficient curve as a function of temperature. The composition of the MCT layer, changed rapidly, becoming HgTe rich when the arsine flow was increased above 350 sccm (500 ppm), and is believed to be due to the pre-reaction of dimethylcadmium with arsine. Isothermal annealing of the layers grown on CdTe has shown that the measured carrier concentration is due to As alone. This is evidenced by the negligible change in the doping concentration between unannealed layers and those annealed for 15 hours at 205°C.

#### ACKNOWLEDGEMENT

The authors would like to thank J. Barthel for technical assistance on this program and P. Magilligan for manuscript preparation. This work was sponsored by the Defense Advanced Research Projects Agency (Contract No. N-00014-85-K-0151), administered through the Office of Naval Research, Arlington, VA. This support is greatly appreciated.

## REFERENCES

1. S.J. Irvine and J.B. Mullin, *J. Cryst. Growth*, 55, 107 (1981).
2. S.K. Ghandhi and I.B. Bhat, *Appl. Phys. Lett.*, 44, 779 (1984).
3. W.E. Hoke, P.J. Lemonias and R. Taczewski, *Appl. Phys. Lett.*, 45, 1092 (1984).
4. J.L. Schmit, *J. Vac. Sci. Technol.*, A3, 89 (1985).
5. W.E. Hoke and P.J. Lemonias, *Appl. Phys. Lett.*, 48, 1669 (1986).
6. S.K. Ghandhi, I.B. Bhat and H. Fardi, *Appl. Phys. Lett.*, 52, 392 (1988).
7. J. Thompson, P. Mackett, L.M. Smith, D.J. Cole-Hamilton and D.V. Shenai-Khatkhate, *J. Cryst. Growth*, 86, 233 (1988).
8. P. Capper, *J. Cryst. Growth*, 57, 280 (1982).
9. M. Brown and A.F.W. Willoughby, *J. Cryst. Growth*, 59, 27 (1982).
10. H.R. Vydyanath, J.A. Ellsworth and C.M. Devaney, *J. Electron. Mat.*, 16, 13 (1987).
11. P.S. Wijewarnasuriya, I.K. Sou, Y.J. Kim, K.K. Mahavadi, S. Sivananthan, M. Bourkerche and J.P. Faurie, *Appl. Phys. Lett.*, 51, 2025 (1987).
12. N.R. Taskar, V. Natarajan, I.B. Bhat and S.K. Ghandhi, *J. Cryst. Growth*, 86, 228 (1988).
13. I.B. Bhat, N.R. Taskar and S.K. Ghandhi, *J. Vac. Sci. Technol.*, A4, 2230 (1986).
14. L.F. Lou and W.H. Frye, *J. Appl. Phys.*, 56, 2253 (1984).
15. J.S. Whiteley, P. Koppel, V.L. Conger and K.E. Owens, *J. Vac. Sci. Tech.*, A6(4), 2804 (1988).
16. C.T. Elliott, I. Melngailis, T.C. Herman and A.G. Foyt, *J. Phys. Chem. Solid*, 33, 1527 (1972).
17. P. Capper, J.J.G. Gosney, C.L. Jones, I. Kenworthy and J.A. Roberts, *J. Cryst. Growth*, 71, 57 (1985).
18. M.H. Kalisher, *J. Cryst. Growth*, 70, 365 (1984).

19. P.P. Debye and E.M. Conwell, Phys. Rev., 93, 693 (1954).
20. C.L. Jones, M.J. T. Quelch, P. Capper and J.J.G. Gosney, J. Appl. Phys., 53, 9080 (1982).



## LEGENDS

Figure 1 Hall mobility and Hall coefficient for an undoped MCT layer grown on GaAs.

Figure 2 Hall coefficient for three MCT layers, with different arsine flow conditions.

Figure 3 Net acceptor concentration as a function of arsine flow. ( ): GaAs substrate, ( $\Delta$ ): CdTe substrate.

Figure 4 (■) Activation energies of arsenic in MCT. The energy of Hg-vacancies is also shown (+) for comparison (Ref. 17).

Figure 5 Hall coefficient for a MCT layer, before and after annealing.

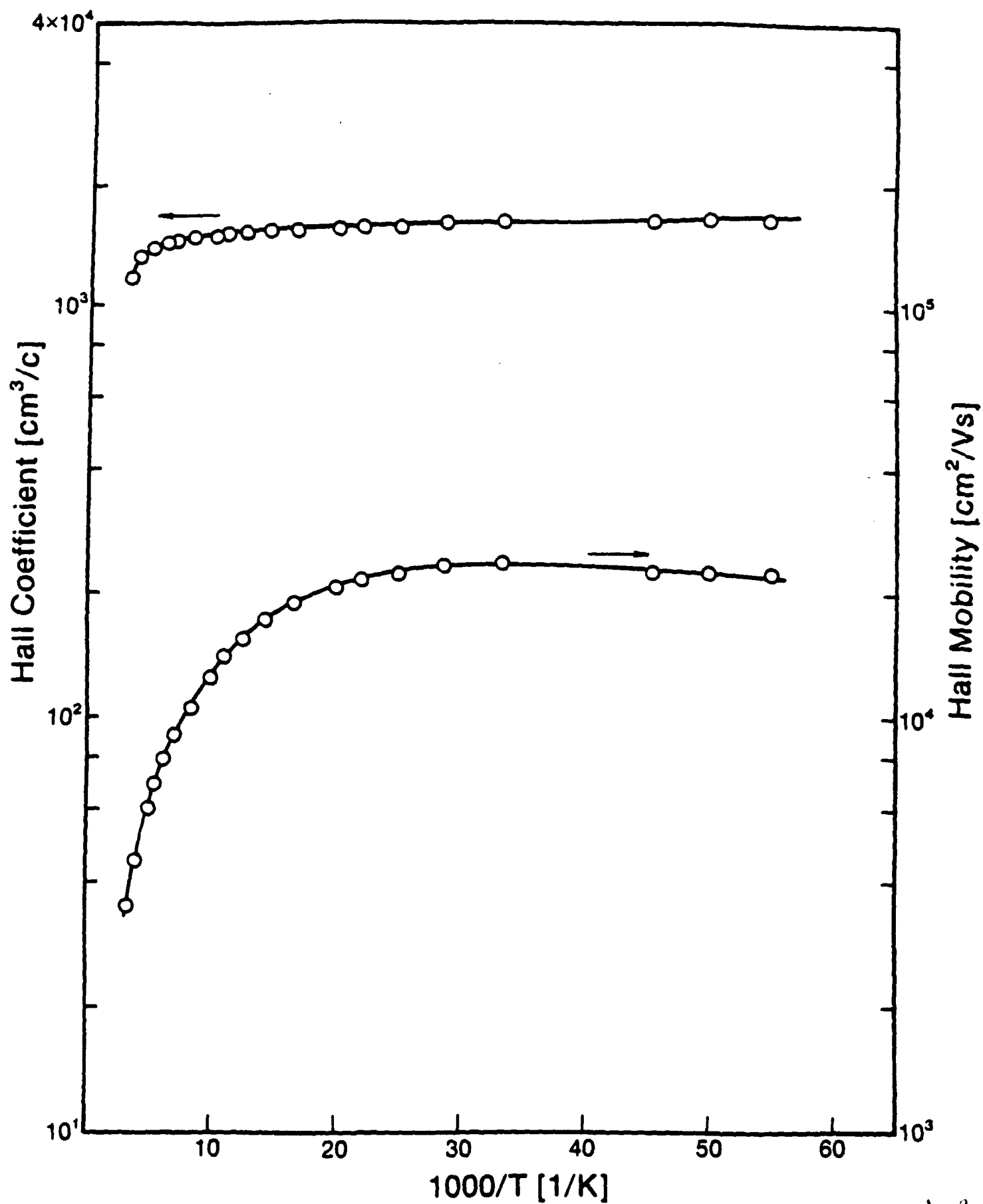


FIG 1  
TASAR  
et al

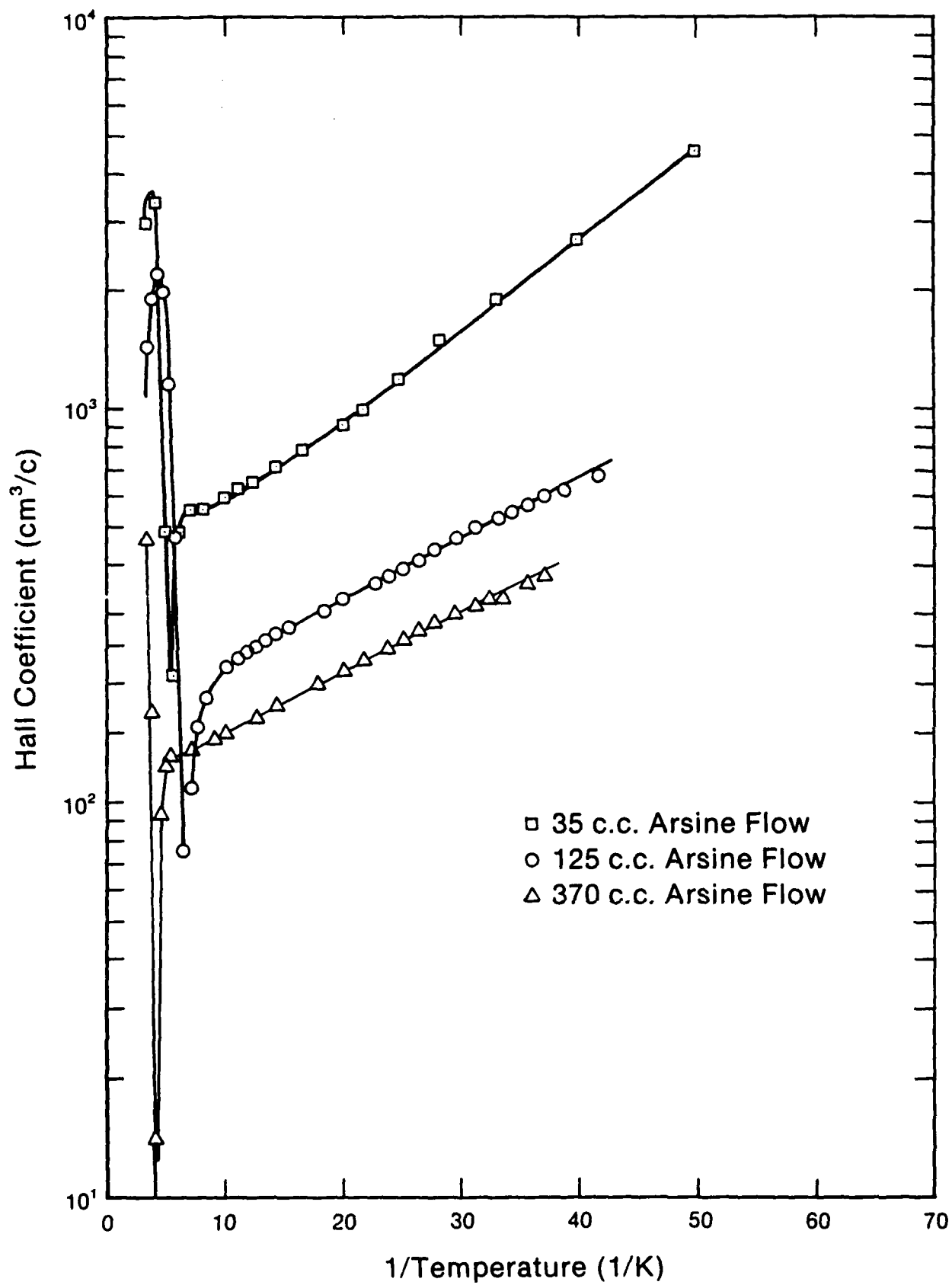


FIG 2  
TASKAR  
al

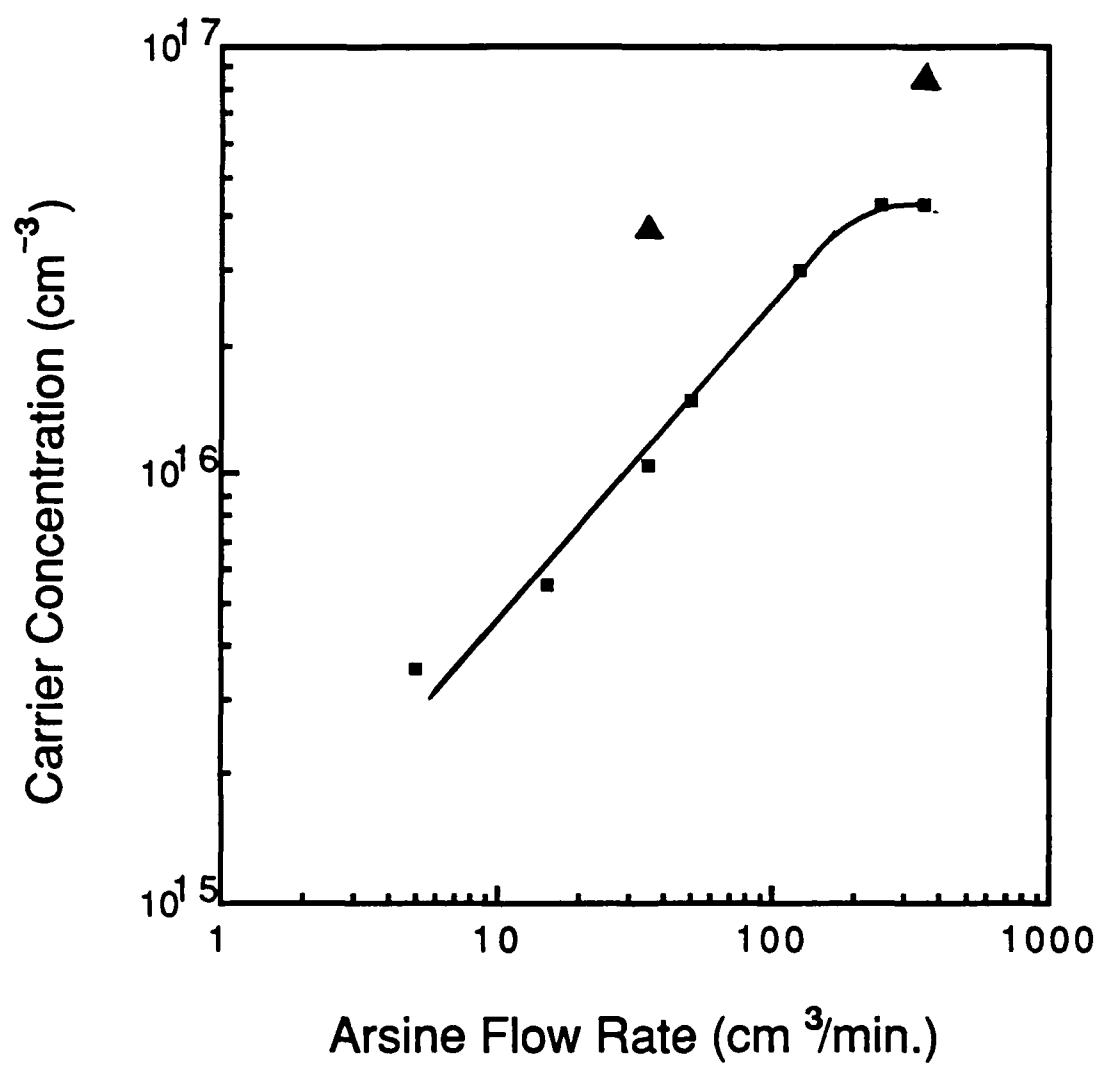


Fig 3  
TASKAR et al

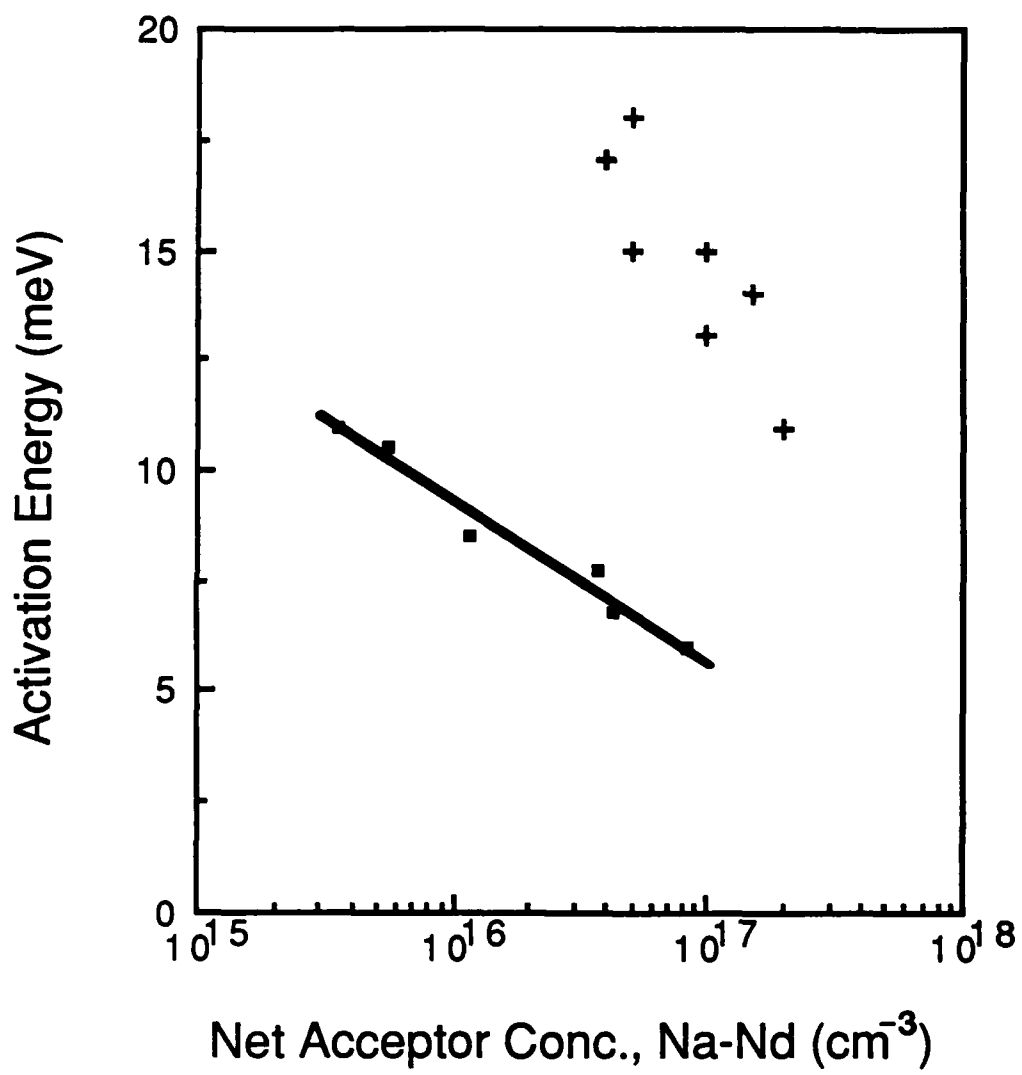


Fig 4  
TASK 72  
etal

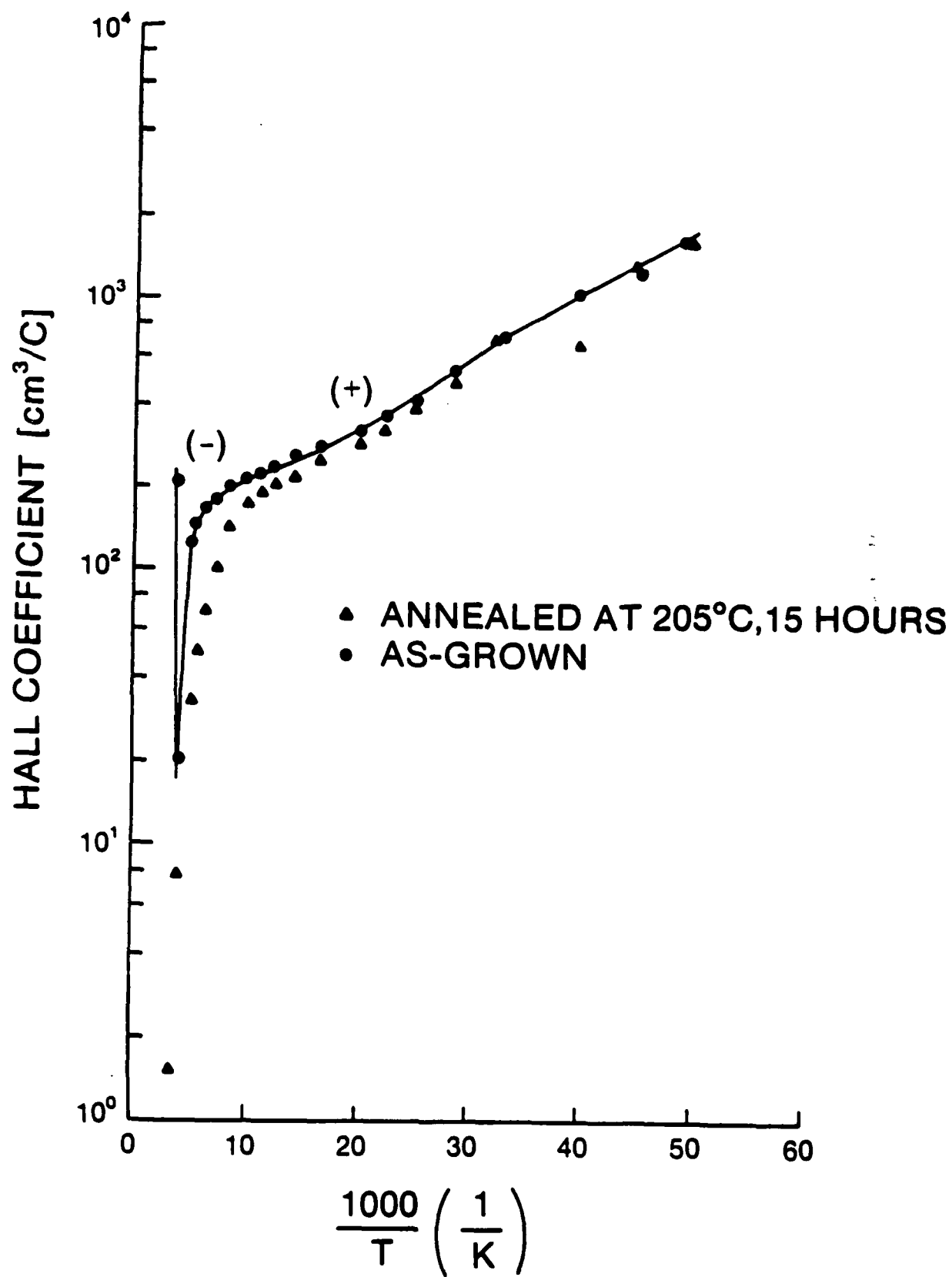


FIG 5  
TASAR  
2/6

APPENDIX-D  
COMPUTER SIMULATION MODEL  
FOR THE EVALUATION OF HALL DATA

The temperature dependence of  $R_H$  and  $\sigma$  was treated in terms of a three carrier model. The three types of carriers were: bulk holes, bulk electrons and surface electrons. It was assumed that surface and bulk layers are in electrical communication. A uniform bulk doping was assumed. In such a case the Hall coefficient of the total layer is given by:

$$R_H = \frac{1}{B} \frac{\sigma_{xy}}{\sigma_{xx}^2 + \sigma_{xy}^2}$$

where

$$\sigma_{xx} = q \left( \frac{n\mu_n}{1 + \mu_n^2 B^2} + \frac{p\mu_p}{1 + \mu_p^2 B^2} + \frac{n_s\mu_s}{1 + \mu_s^2 B^2} \right)$$

and

$$\sigma_{xy} = qB \left( \frac{-n\mu_n^2}{1 + \mu_n^2 B^2} + \frac{p\mu_p^2}{1 + \mu_p^2 B^2} - \frac{n_s\mu_s^2}{1 + \mu_s^2 B^2} \right)$$

Here,  $n$  and  $p$  represent the bulk electron and hole concentrations, and  $n_s$  represents the average concentration (sheet concentration,  $N_s$ , divided by the epilayer thickness) of the surface electrons.  $\mu_n$ ,  $\mu_p$ , and  $\mu_s$  represent the corresponding mobilities. The effect of light holes is ignored in these calculations. In the case of p-type layers, the bulk carrier concentrations were calculated by solving for  $p$  from the following charge balance relation:

$$p = n_i^2/p - N_D + N_A / [1 + 4(p/N_v) \exp(E_A/kT)]$$

where  $N_v = 2 \times 10^{15} T^{3/2}$

Here  $N_A$  is the acceptor concentration and  $N_D$  is the donor concentration.  $N_v$  is the effective density of states at the valence band edge. The acceptors were taken to be singly ionized with an ionization energy of  $E_A$ . In the case of n-type layers, as there is no donor freeze-out, the electron concentration is obtained using the simpler relation:

$$n = \frac{(N_D - N_A) + \{(N_D - N_A)^2 + 4n_i^2\}^{1/2}}{2}$$

The surface electron concentration was assumed to be independent of the temperature.

The hole mobility was assumed to be limited by lattice scattering (with a  $T^{-1.9}$  dependence), and low temperature alloy/ionized impurity scattering, which was assumed to be temperature independent. The bulk electron mobility was calculated by multiplying the hole mobility by the inverse of the effective mass ratio. For the surface electrons, an additional, temperature independent, surface scattering limited mobility was also included. These relations are summarized below:

$$\mu_p = 1/[1/\{\mu_{300}(300/T)^{1.9}\} + 1/\mu_{p0}]$$

$$\mu_n = (m_h^*/m_e^*)\mu_p$$

$$\mu_s = 1/(1/\mu_n + 1/\mu_{s0})$$

Here,  $\mu_{300}$  is the lattice scattering limited mobility of holes at 300K, and  $\mu_{p0}$  is hole mobility in the low temperature limit, in the absence of lattice scattering. Similarly,  $\mu_{s0}$  is the mobility of the surface electrons in the low temperature limit. In practice, the hole mobility does not increase steadily with decreasing temperature; instead it peaks around 40-20K [19]. However, for simplicity, the above model for mobility was assumed. For analyzing the Hall data, the composition and thickness of the layer were measured using an FTIR. Then, the values  $N_A$ ,  $N_D$ ,  $E_A$ ,  $N_S$ ,  $\mu_0$ , and  $\mu_S$  were varied and optimized till a reasonable fit to the experimental  $R_H$  and  $\sigma$  is obtained. In the case of p-type layers,



the fit was more sensitive to the value of  $(N_A - N_D)$  rather than their individual values. As a result,  $N_D$  was chosen to be around  $5 \times 10^{14}/\text{cc}$ , as determined from the residual donor concentration in the fully annealed layers. Using this value of  $N_D$ ,  $N_A$  was optimized. In the case of n-type layers, the net donor concentration can be determined by measuring the electron concentration in the layer at low temperatures, since the donors do not undergo thermal freeze-out. However, the presence of surface electrons can lead to an overestimation of the actual bulk donor concentration, unless care is taken to account for them. The actual bulk and surface electron concentration and mobility in these n-type layers were determined by analyzing the variation in the  $R_H$  of the layer with B-field, since this approach is more convenient and accurate compared to the technique described previously. For an n-type layer having a surface electron accumulation layer the  $R_H$  is given by:

$$R_H = (C_1 + C_2 B^2) / (1 + C_3 B^2)$$

where

$$C_1 = -q \cdot (\mu_n^2 n + \mu_s^2 n_s) / \sigma^2$$

$$C_2 = -q \cdot \mu_n^2 \mu_s^2 (n + n_s) / \sigma^2$$

$$C_3 = q^2 \cdot \mu_n^2 \mu_s^2 (n + n_s)^2 / \sigma^2$$

and

$$\sigma = q \cdot (n \mu_n + n_s \mu_s)$$

Here  $n$  is the bulk electron concentration and  $n_s$  is the average concentration (sheet electron concentration divided by the total epi-layer thickness) of the surface electrons.  $\mu_n$

and  $\mu_s$  are the corresponding mobilities.  $R_H$  was measured at different values of B-field and from this data the various bulk and surface parameters were evaluated. This variable B-field approach can be used for analyzing the p-type layers as well. However, due to the low mobility of the bulk holes, very high B-fields are required for successfully analyzing light p-type layers having surface inversion layers. In addition, due to the freeze-out of holes, the actual acceptor concentration and the acceptor activation energy can be evaluated only by analyzing the temperature dependence of the hole concentration. As a result, p-type layers were exclusively analyzed by studying the temperature dependence of the  $R_H$  and  $\sigma$ .